The Abdus Salam
International Centre
for Theoretical Physics

United Nations
Educational, Scientific and
Cultural Organization

IAEA
International Atomic Energy Agency

2455-3

Workshop on Portable X-ray Analytical Instruments for Cultural Heritage

29 April - 3 May, 2013

External-beam IBA methods for non-destructive analysis of Cultural Heritage Artefacts

Massimo Chiari
I.N.F.N., Firenze
Italy

Strada Costiera, 11 - 34151 - Trieste - Italy • Tel. +39 0402240111 • Fax. +39 040224163 • sci_info@ictp.it • www.ictp.it
ICTP is governed by UNESCO, IAEA, and Italy, and it is a UNESCO Category 1 Institute

External-beam IBA methods for non-destructive analysis of Cultural Heritage arefacts

Massimo Chiari / *I.N.F.N. Florence*

chiari@fi.infn.it

max0068

INFN LABEC Laboratorio di Tecniche Nucleari per i Beni Culturali - Firenze

Joint ICTP-TWAS Workshop on "Portable X-ray Analytical Instruments for Cultural Heritage"
Trieste (Italy), 29 April - 3 May 3,2013

Outline

- Introduction to Ion Beam Analysis
- External beams
- IBA applications to Cultural Heritage
- Essential bibliography

Ion Beam Analysis techniques

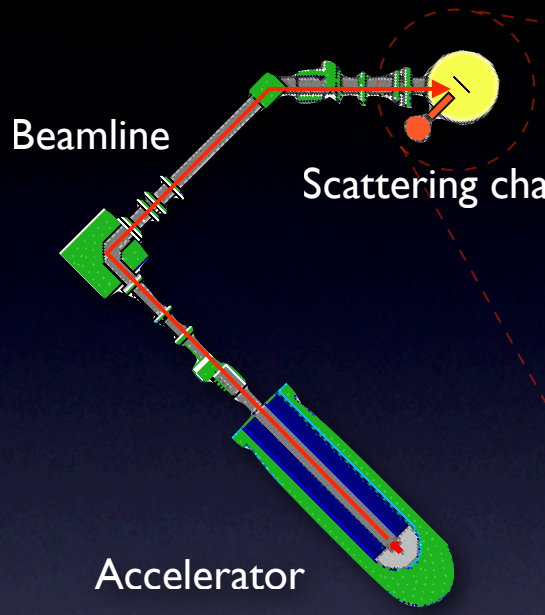

Beam IN	Beam OUT	Analytical technique
ion	ion	RBS, NRA
ion	target	ERDA, SIMS, SNMS
ion	X-ray	PIXE
ion	Gamma-ray	PIGE, Activation Analysis
ion	hν	Ionoluminescence (IL)

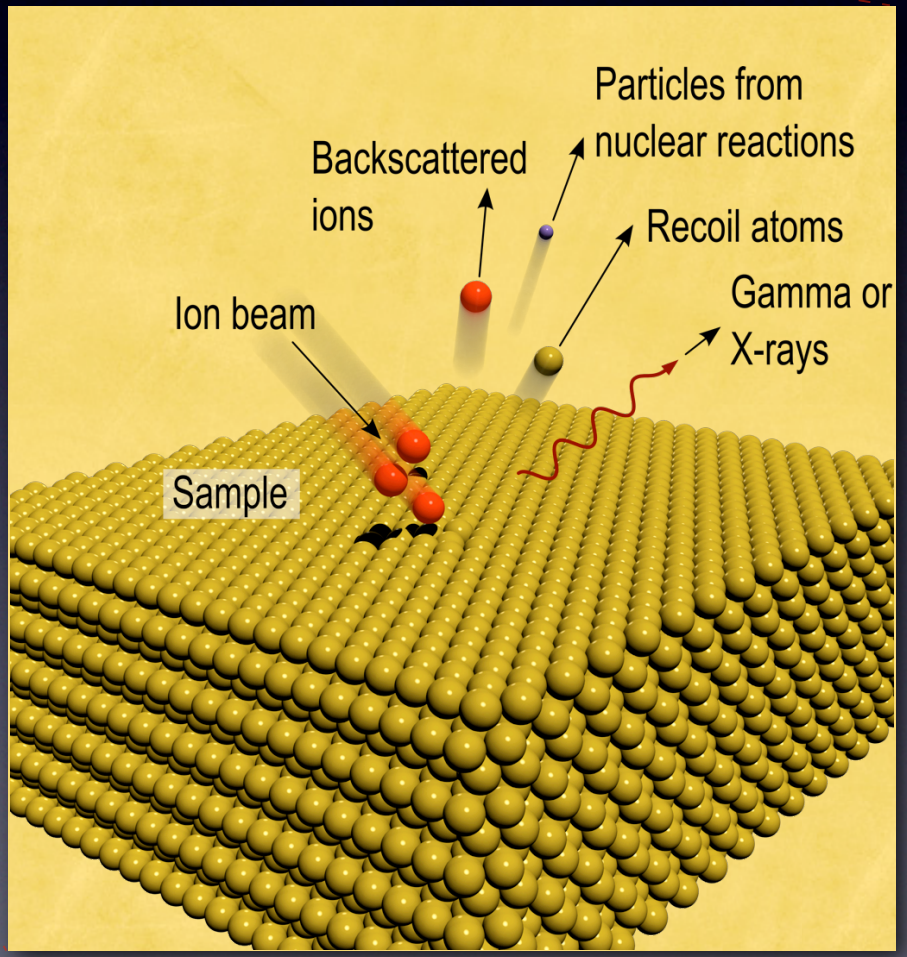

General features of IBA

- Multielemental
- Quantitative analysis ("traceability")
- High sensitivity (1-100 ppm in at/cm^3; 10^{11}-10^{12} in at/cm^2)
- Surface analysis (10 Å - 10 µm)
- Depth profiling
- Non-destructive
- No sample pre-treatment
- Microanalysis (lateral resolution <1 µm)
- 2D mapping

Stopping power

The "stopping power" (the energy lost per unit lenght, dE/dx) is a macroscopic and measurable quantity, describing the average interaction of the ion with the material:

$$-\frac{dE}{dx} = \frac{4\pi}{m_e c^2} \cdot \frac{nz^2}{\beta^2} \cdot \left(\frac{e^2}{4\pi\varepsilon_0}\right)^2 \cdot \left[\ln\left(\frac{2m_e c^2 \beta^2}{I \cdot (1-\beta^2)}\right) - \beta^2\right]$$

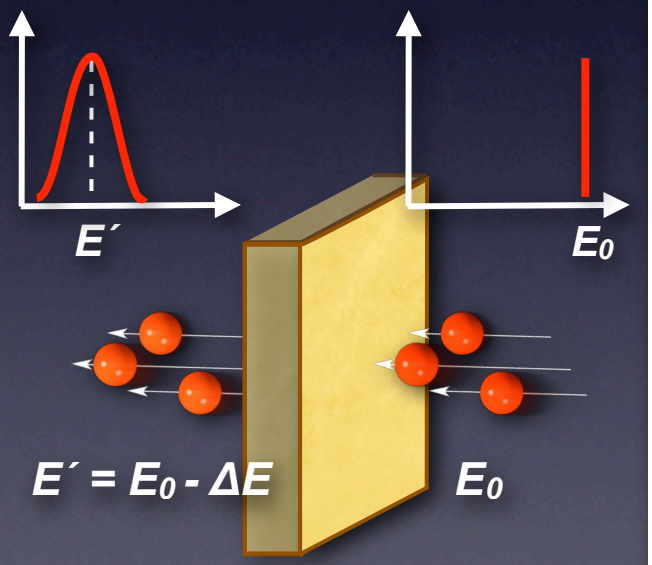

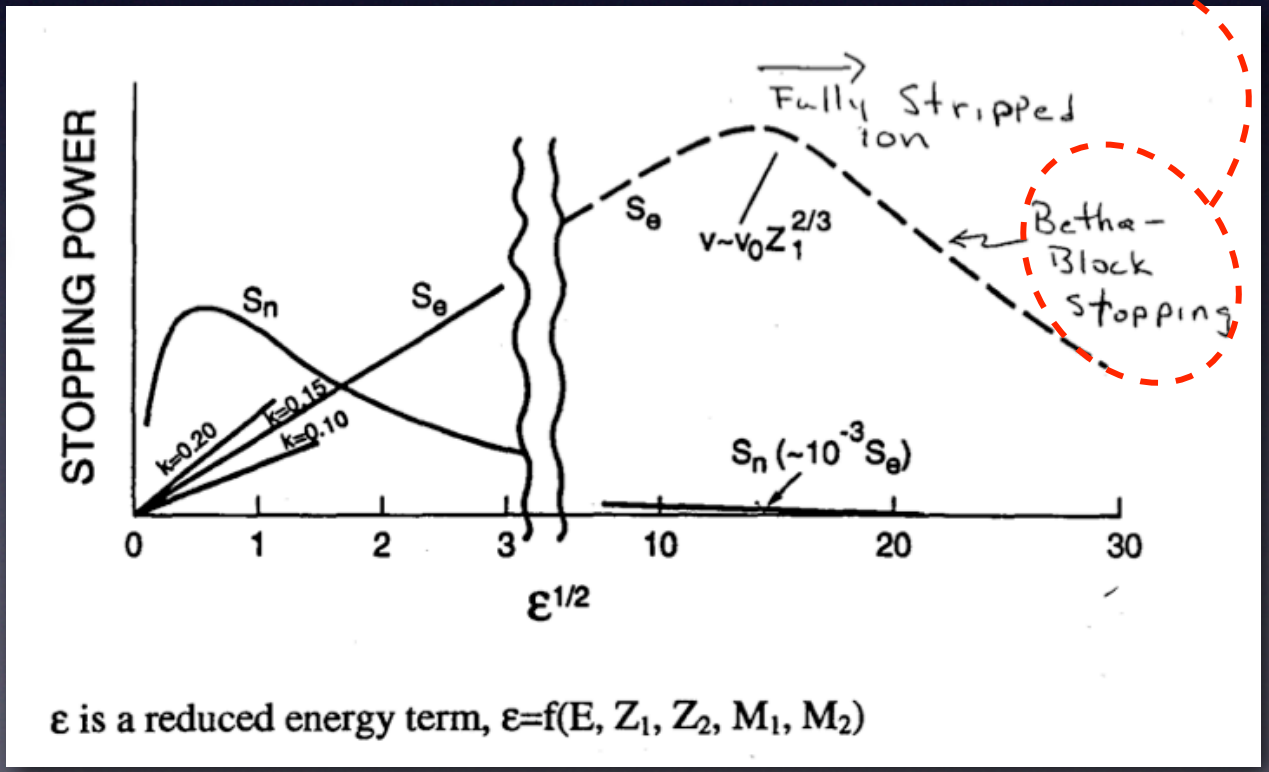

ε is a reduced energy term, ε=f(E, Z_1, Z_2, M_1, M_2)

PIXE

Particle Induced X-ray Emission

Emission of characterisic X-rays following ioniziation from incident ions

Z>10

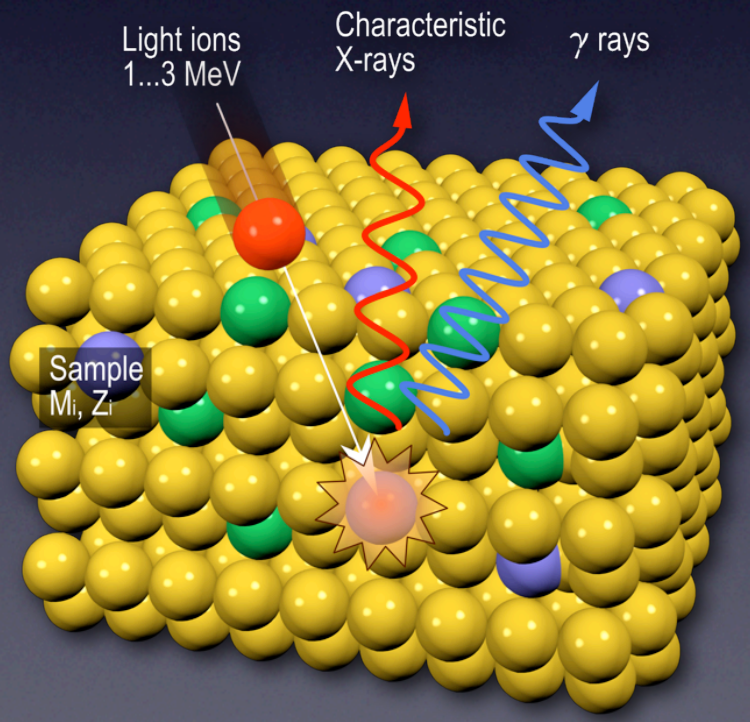

Energy of characteristic X-rays

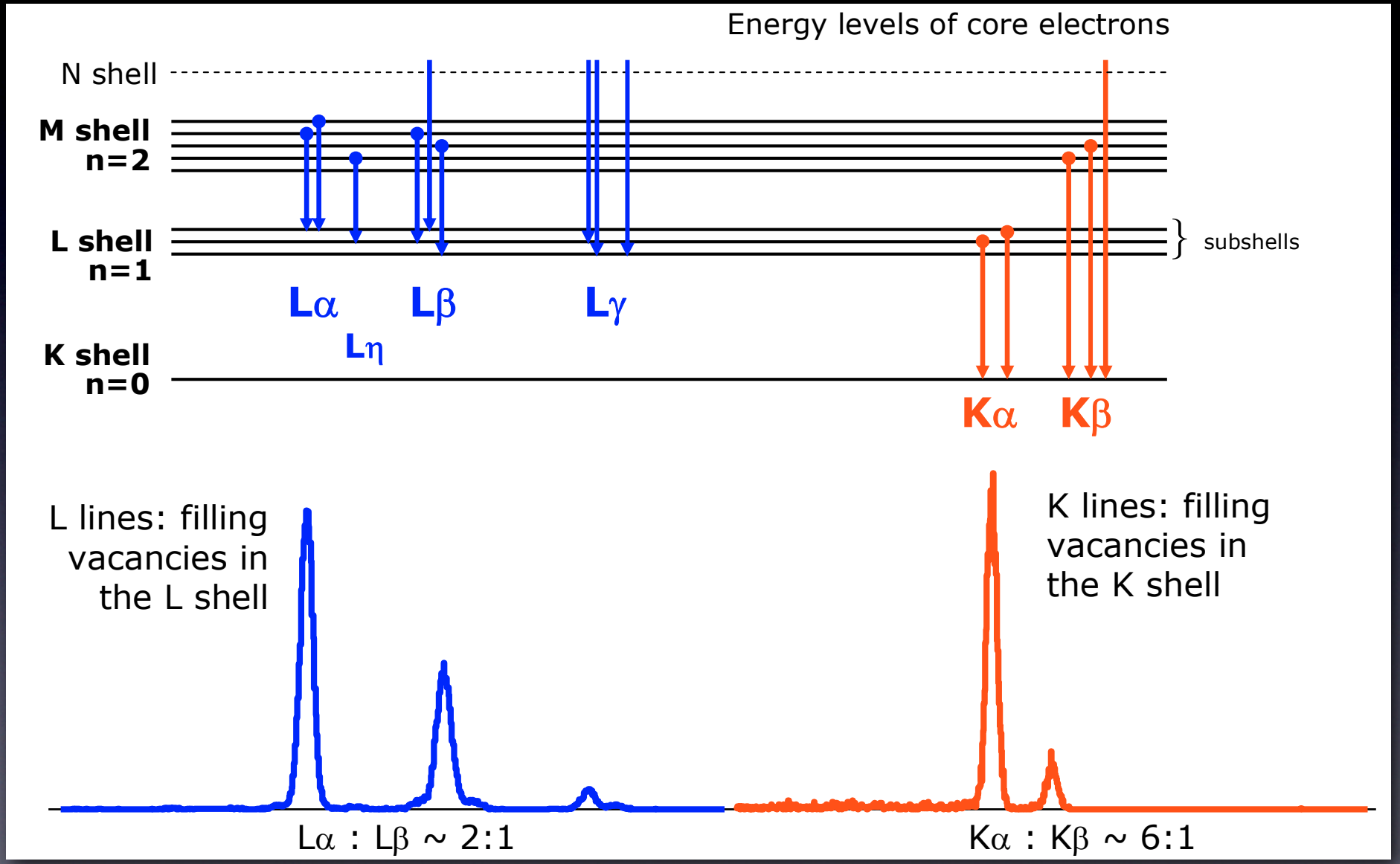

Energy of characteristic X-rays

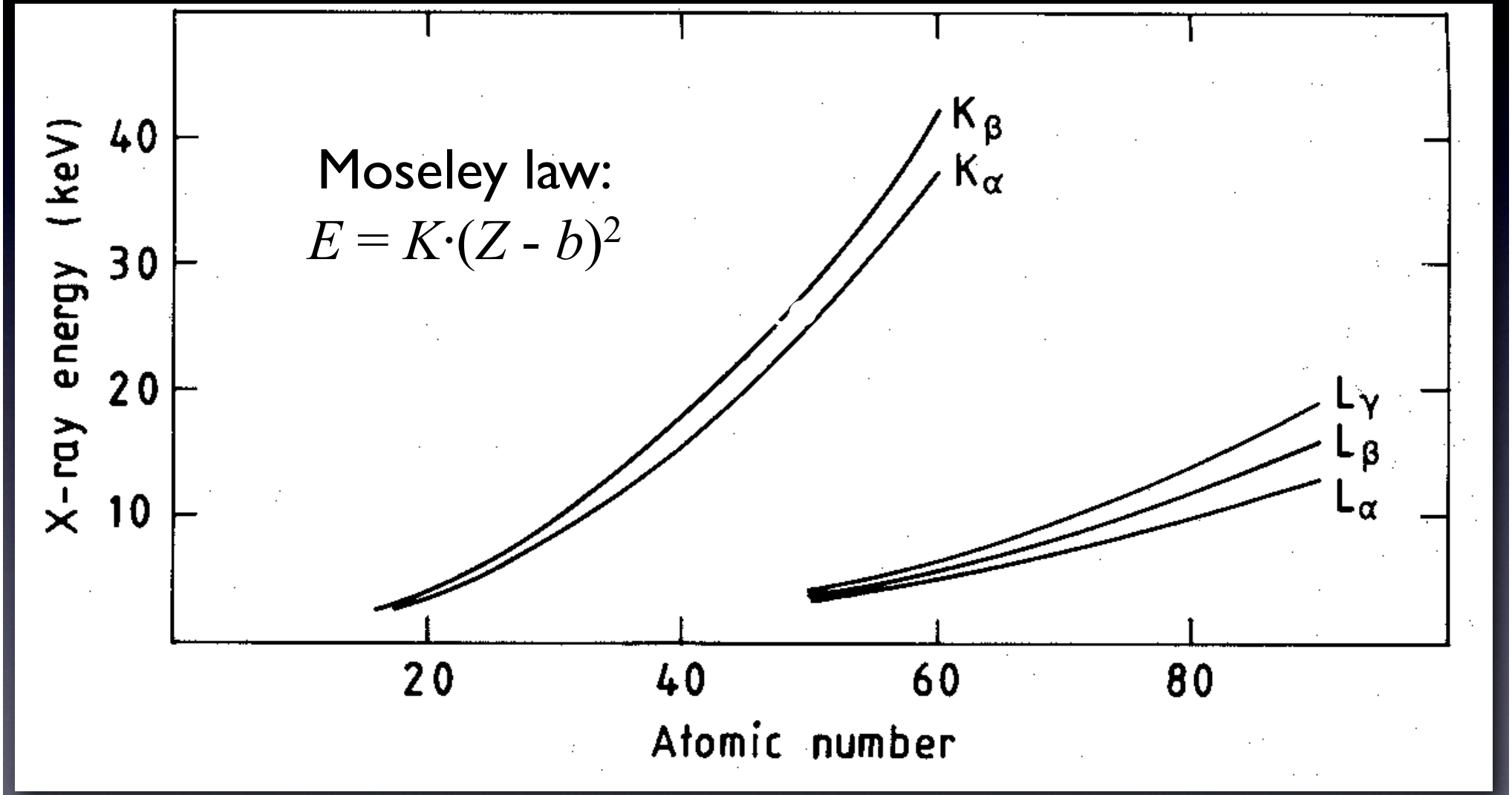

X-ray production cross sections

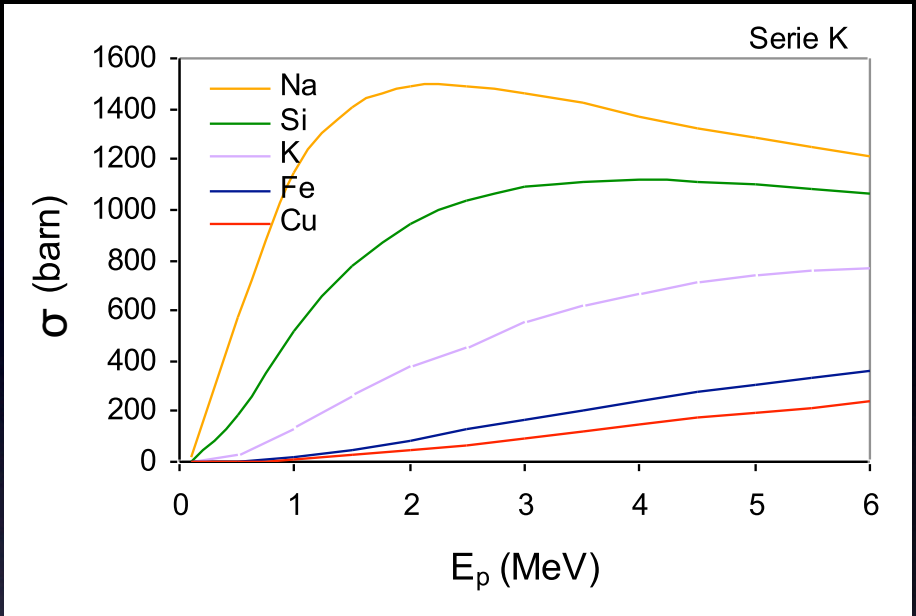

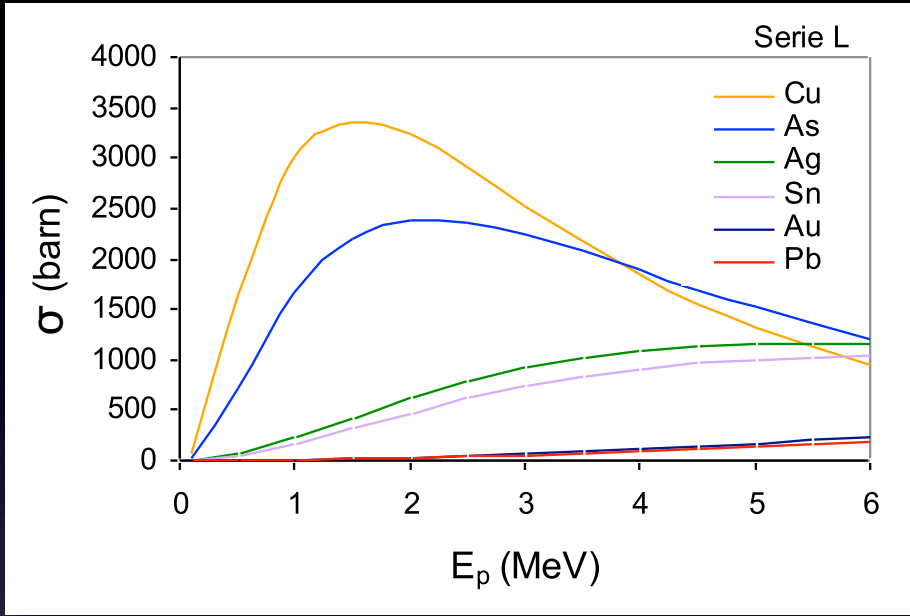

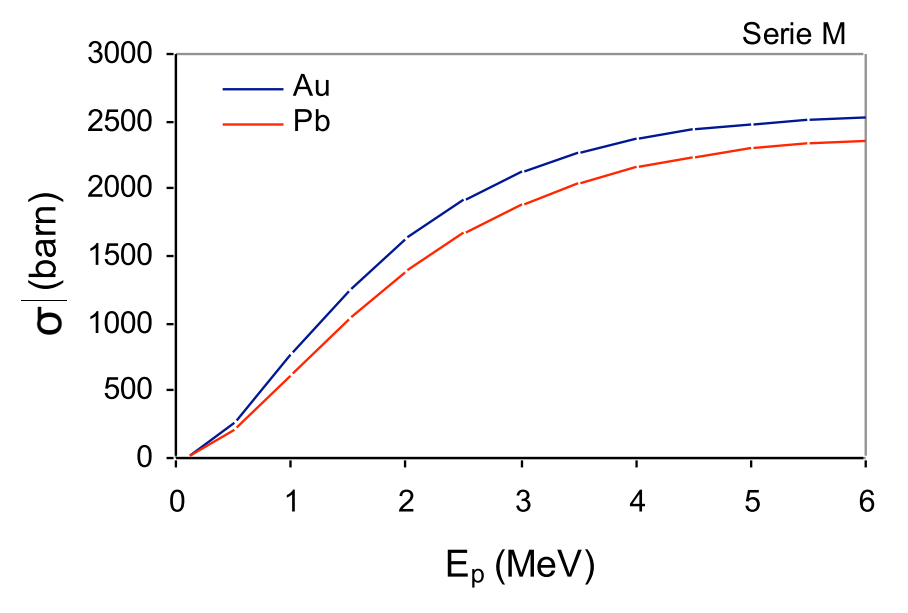

Adavantages of PIXE

- very fast, high-sensitivity, **non-destructive** analysis
- **quantitative** analysis
- minimum energy of detected X-rays tipically ~1 keV

➡ *all the elements with $Z \geq 11$ are quantifible simultaneously*

Limitations of PIXE

- no information on the organic components
- no direct information on chemical bonds

but… hypothesis on stoicheometry through quantitative and multielemental anaylisis

- no direct information on the stratigrapgy and the depth distribution of the elements

but… Differential PIXE

Example of PIXE spectra

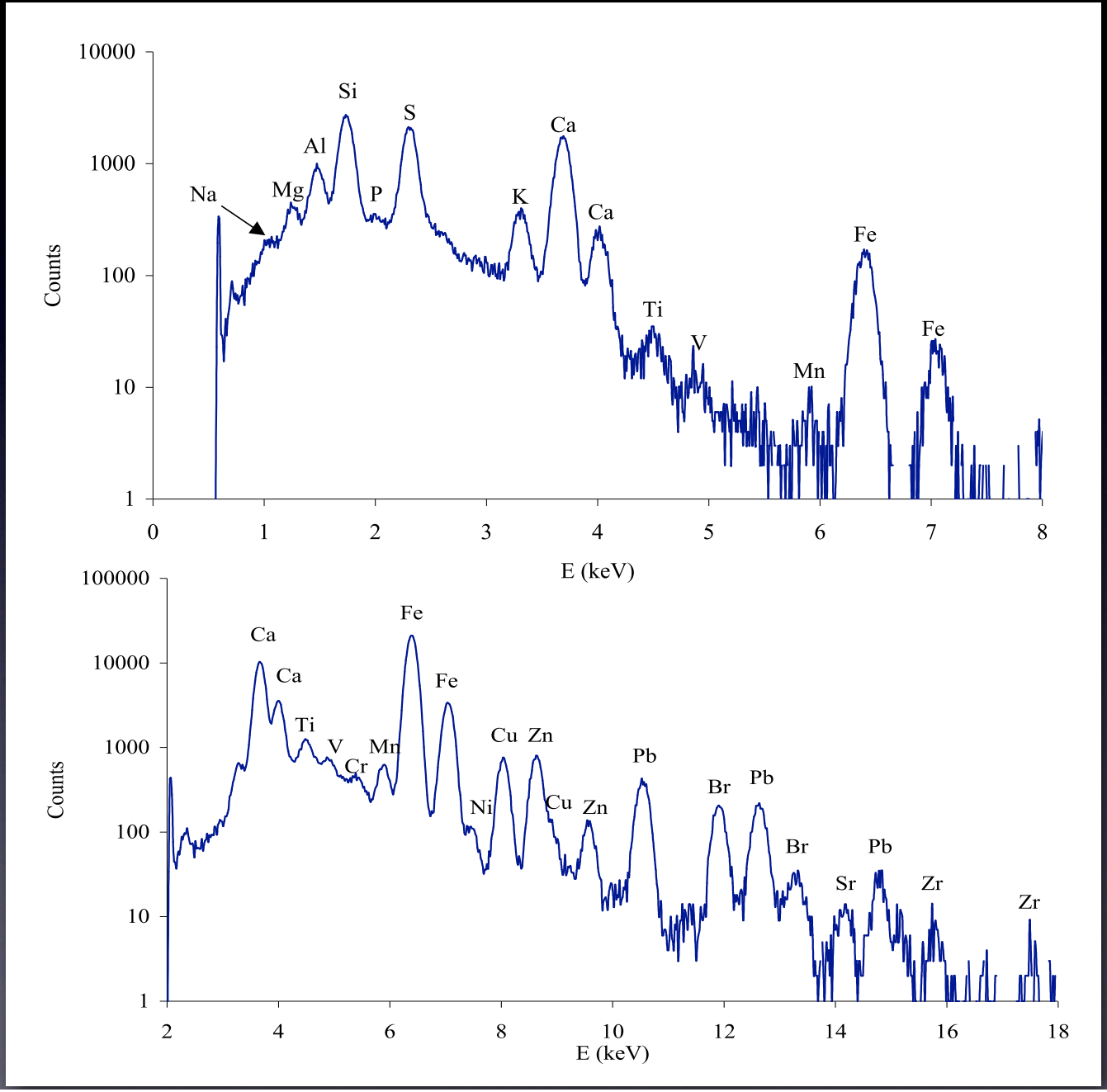

Quantitative analysis (thin target)

$$Y_0(Z) = N_P \cdot N_Z \cdot t \cdot \sigma_{Z,E0} \cdot (\alpha_Z \cdot \varepsilon_Z \cdot \Delta\Omega/4\pi)$$

$$Y_0(Z) = (Q/e)(N_A/A)(\rho_Z t) \cdot \sigma_{Z,E0} \cdot (\alpha_Z \cdot \varepsilon_Z \cdot \Delta\Omega/4\pi)$$

defining $\eta_Z = (1/e)(N_A/A) \cdot \sigma_{Z,E0} \cdot (\alpha_Z \cdot \varepsilon_Z \cdot \Delta\Omega/4\pi)$

$$Y_0(Z) = \eta_Z \cdot Q \cdot (\rho_Z t)$$

$$\boldsymbol{(\rho_Z t) = Y_0(Z) / (\eta_Z \cdot Q)}$$

Thick targets

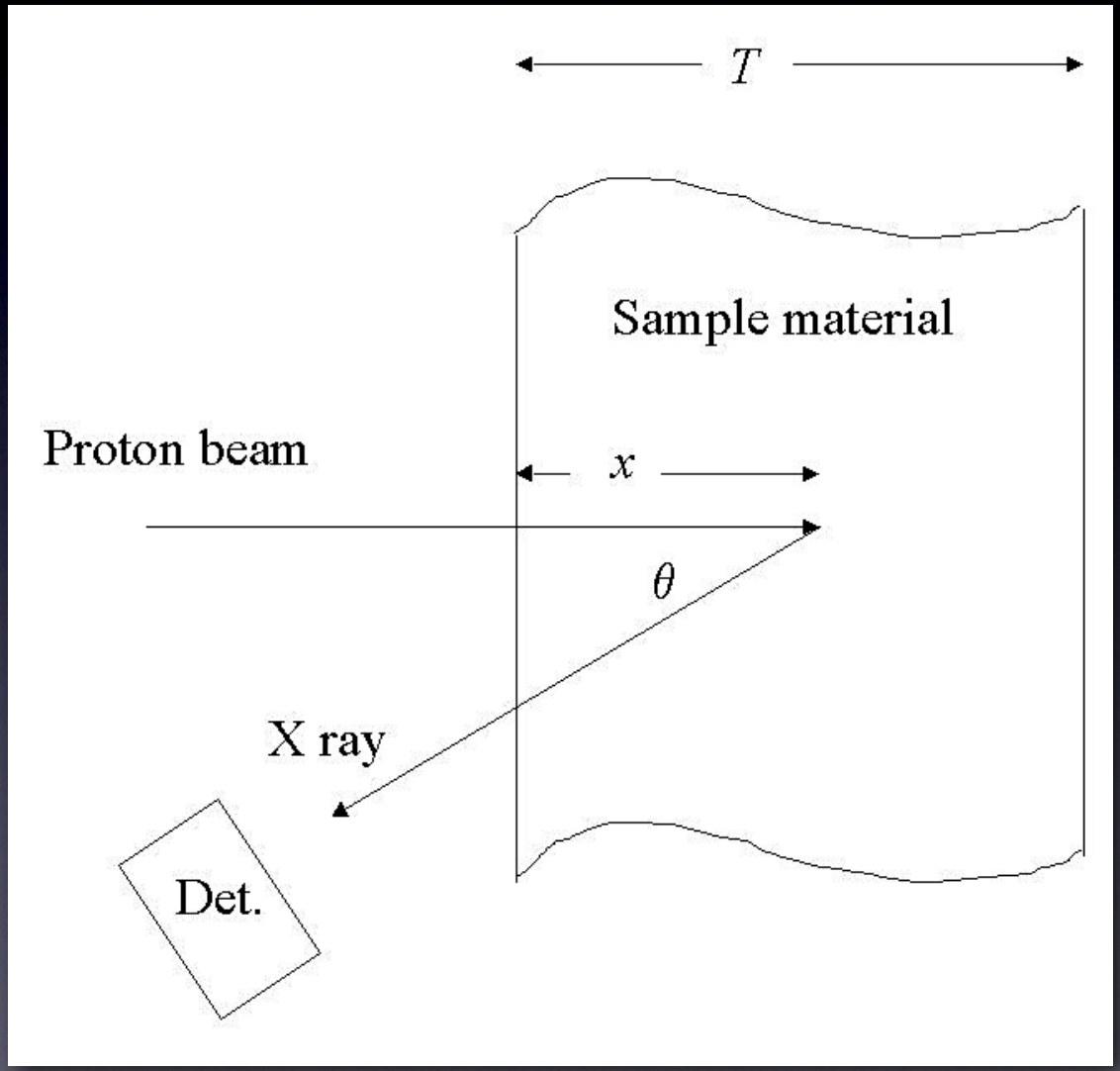

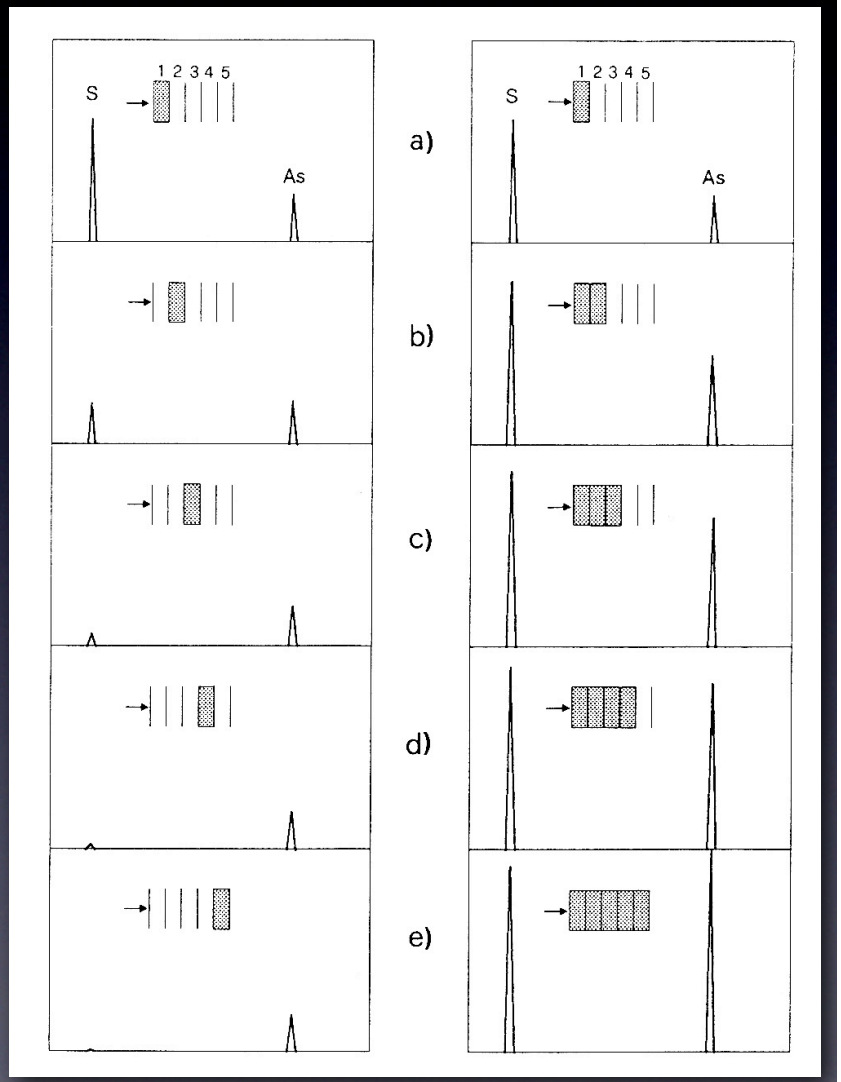

Quantitative analysis (thick targets)

$$Y(Z) = (Q/e)(N_A/A)(\alpha_Z \cdot \varepsilon_Z \cdot \Delta\Omega/4\pi) \cdot \rho_Z \int_0^T \sigma_{Z,E} \cdot \exp(-\mu \cdot x/\cos\theta) \cdot dx$$

$$Y(Z) = (Q/e)(N_A/A)(\alpha_Z \cdot \varepsilon_Z \cdot \Delta\Omega/4\pi)(\rho_Z/\rho) \int_{E_0}^{E_F} \sigma_{Z,E} \cdot \exp(-\mu \cdot x/\cos\theta) \cdot dE/S(E)$$

$$F(Z) = Y_0(Z)/Y(Z) = \frac{\rho \cdot T \cdot \sigma_{Z,E0}}{\int_{E_0}^{E_F} \sigma_{Z,E} \cdot \exp(-\mu \cdot x/\cos\theta) \cdot dE/S(E)}$$

$$\boxed{(\rho_Z t) = F(Z) \cdot Y(Z) / (\eta_Z \cdot Q)}$$

2-detectors PIXE set-up

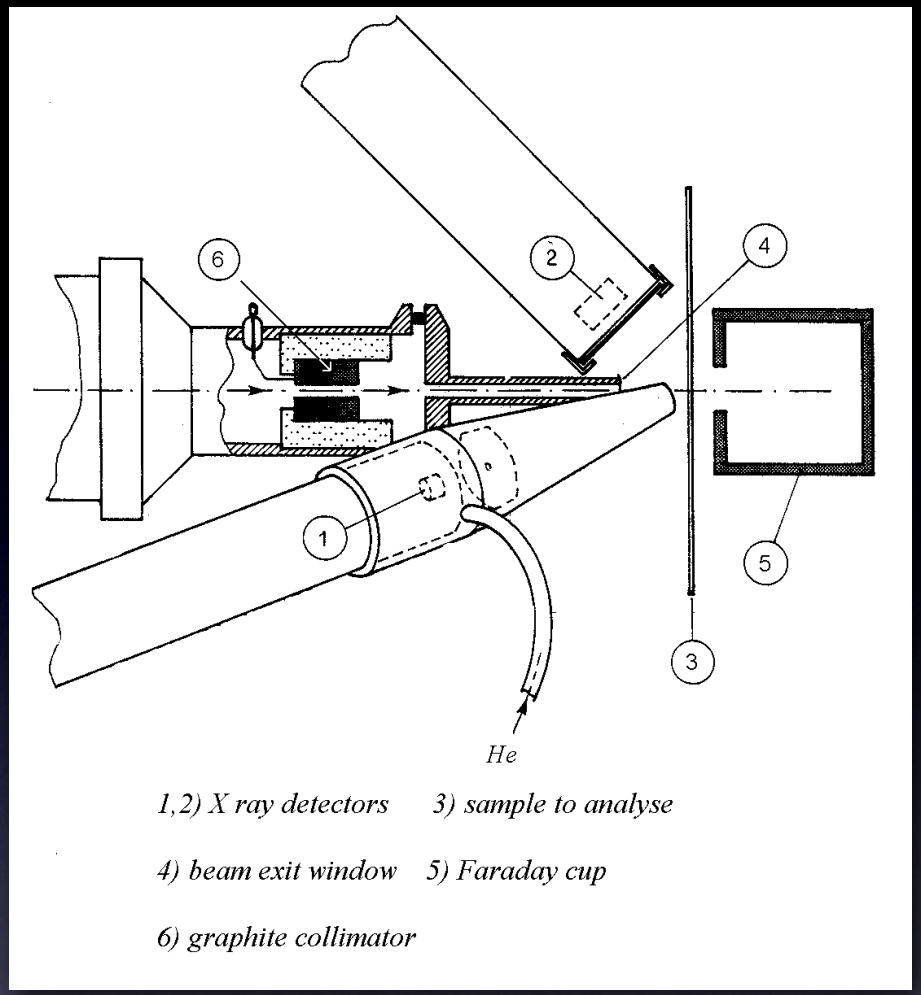

1,2) X ray detectors *3) sample to analyse*

4) beam exit window *5) Faraday cup*

6) graphite collimator

Target	X-rays	What is needed	Detector features
Low-Z elements	Low energy High cross sections	Minimum dead layers Small solid angles	Thin entrance window Small active area
Medium-high-Z elements	High energy Low cross sections	Large solid angles Efficiency	Large active area Large active thickness

Detection efficiency for a 2-detectors PIXE set-up

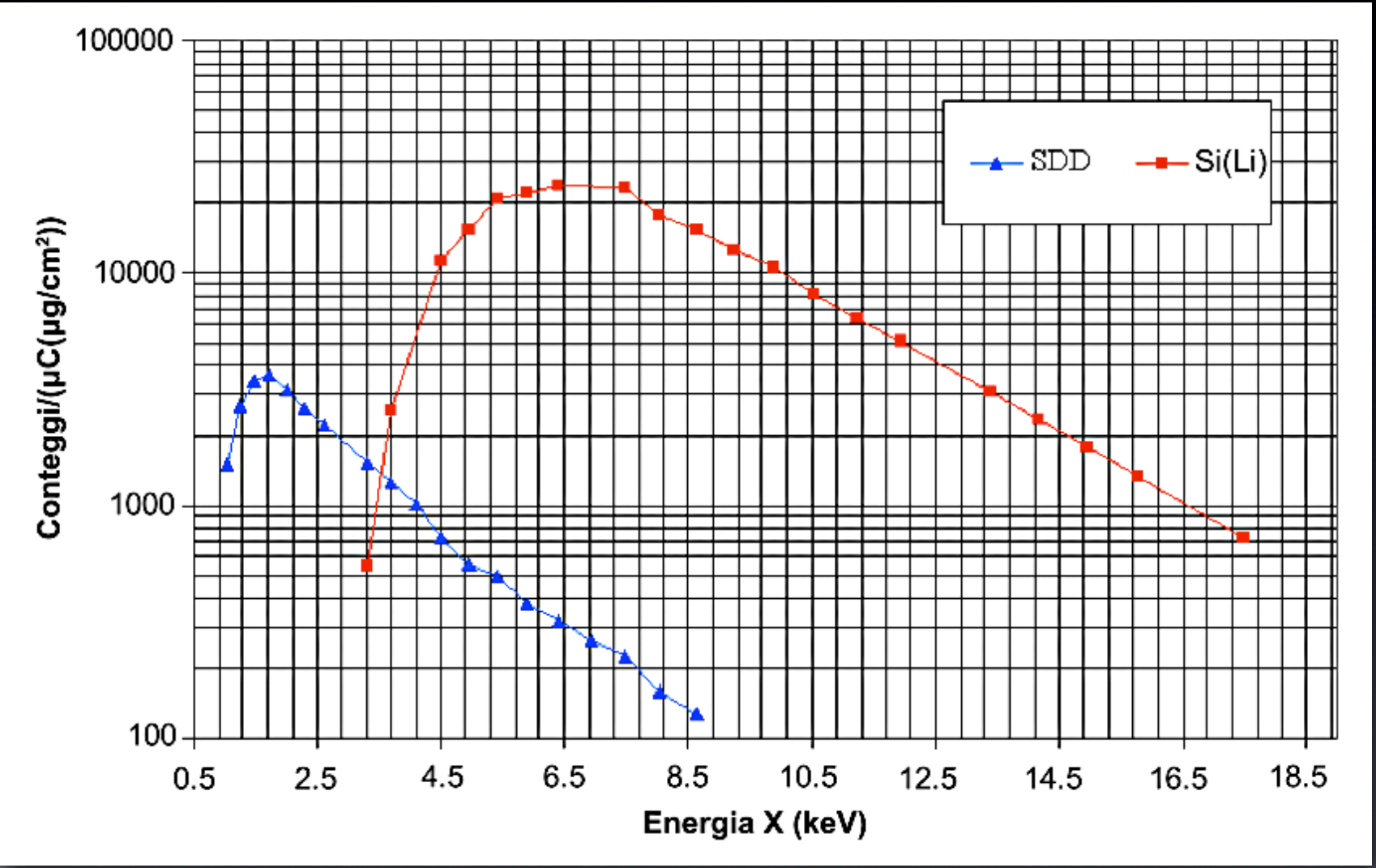

PIGE

Particle Induced Gamma-ray Emission

Prompt emission of gamma-rays during the ion beam irradiation

Li, B, F, Na, Al...

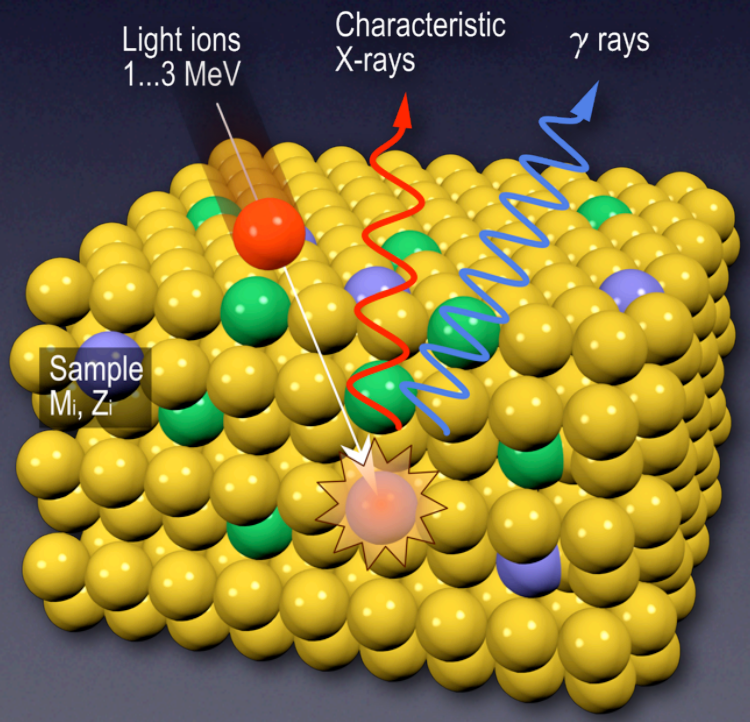

Nuclear reactions with prompt emission of gamma -rays

Radiative capture (direct reaction)	$a + A \rightarrow B^* \rightarrow B + \gamma$	$^{27}Al(p,\gamma)^{28}Si$
Inelastic scattering	$a + A \rightarrow A^* + a'$ $\searrow$ $A + \gamma$	$^{27}Al(p,p'\gamma)^{27}Al$
Rearrangement collisions	$a + A \rightarrow C^* + c$ $\searrow$ $C + \gamma$	$^{27}Al(p,\alpha\gamma)^{24}Mg$

List of proton-induced reaction

Element	E_γ (keV)	Nuclear origin	Transition	Detection limit (%)	Possible interferences
Li	429	$^{7}Li(p,n\gamma)^{7}Be$	429 → 0	0.01	As(427), B(429)
	478	$^{7}Li(p,p'\gamma)^{7}Li$	478 → 0	5×10^{-4}	Be(478), Mn(478)
Be	415	$Be^{9}(p,\gamma)B^{10}$	2154 → 1740		Ag(415)
	718	$Be^{9}(p,\gamma)B^{10}$	718 → 0		B(718)
	1023	$Be^{9}(p,\gamma)B^{10}$	1740 → 718		Ti(1022)
	1437	$Be^{9}(p,\gamma)B^{10}$	3590 → 2150		
	3562	$Be^{9}(p,\alpha\gamma)Li^{6}$	3562 → 0	0.1	
B	429	$^{10}B(p,\alpha\gamma)^{7}Be$	429 → 0		As(427), Li(429)
	478	$^{10}B(p,\alpha\gamma)^{7}Be \rightarrow {}^{7}Li$	478 → 0		Li(478), Mn(478)
	718	$^{10}B(p,p'\gamma)^{10}B$	718 → 0		Be(718)
	2124	$^{10}B(p,p'\gamma)^{10}B$	2124 → 0	5×10^{-3}	
	4433	$^{11}B(p,\gamma)^{12}C$	4433 → 0		N(4433)

List of proton-induced reaction

Element	E_γ (keV)	Nuclear origin	Transition	Detection limit (%)	Possible interferences
C	2357	$^{12}C(p,\gamma)^{13}N$	2357 → 0	1	
N	1400	$^{14}N(p,\gamma)^{15}O$			Cr(1400)
	4433	$^{15}N(p,\alpha\gamma)^{12}C$	4433 → 0		B(4433)
O	110	$^{18}O(p,\gamma)^{19}F$	110 → 0		F(110), W(111)
	197	$^{16}O(p,\gamma)^{19}F$	197 → 0		F(197), Co(197), Ni(197), Ga(197), Ti(199), Ge(199)
	496	$^{16}O(p,\gamma)^{17}F$	496 → 0	5	Ga(493)
F	110	$^{19}F(p,p'\gamma)^{19}F$	110 → 0	2×10^{-4}	O(110), W(111)
	197	$^{19}F(p,p'\gamma)^{19}F$	197 → 0	5×10^{-5}	Co(197), Ni(197), Ga(197) Ti(199), Ge(199), O(197)
Na	439	$^{23}Na(p,p'\gamma)^{23}Na$	439 → 0	10^{-3}	Se(439)
	1368	$^{23}Na(p,\gamma)^{24}Mg$	1368 → 0		Mg(1368), Al(1368)
	1633	$^{23}Na(p,\alpha\gamma)^{20}Ne$	1633 → 0		

List of proton-induced reaction

Element	E_γ (keV)	Nuclear origin	Transition	Detection limit (%)	Possible interferences
Mg	170	$^{26}Mg(p,\gamma)^{27}Al$	1014 → 844		Al(170)
	390	$^{25}Mg(p,p'\gamma)^{25}Mg$	975 → 585		
	585	$^{25}Mg(p,p'\gamma)^{25}Mg$	585 → 0	5×10^{-3}	
	844	$^{26}Mg(p,\gamma)^{27}Al$	844 → 0		Al(844)
	975	$^{25}Mg(p,p'\gamma)^{25}Mg$	975 → 0		
	1014	$^{26}Mg(p,\gamma)^{27}Al$	1014 → 0		Ti(1012), Al(1014)
	1368	$^{24}Mg(p,p'\gamma)^{24}Mg$	1368 → 0		Na(1368), Al(1368)
Al	170	$^{27}Al(p,p'\gamma)^{27}Al$	1014 → 844		Mg(170)
	844	$^{27}Al(p,p'\gamma)^{27}Al$	844 → 0	2×10^{-3}	Mg(844)
	1014	$^{27}Al(p,p'\gamma)^{27}Al$	1014 → 0	5×10^{-3}	Ti(1012), Mg(1014)
	1368	$^{27}Al(p,\alpha\gamma)^{24}Mg$	1368 → 0		Na(1368), Mg(1368)
	1779	$^{27}Al(p,\gamma)^{28}Si$	1779 → 0		Si(1779), P(1779)
Si	1273	$^{29}Si(p,p'\gamma)^{29}Si$	1273 → 0	3	
	1779	$^{28}Si(p,p'\gamma)^{28}Si$	1779 → 0		Al(1779), P(1779)

PIGE cross sections

The cross sections are the superimposition of resonances (Breit-Wigner) on a continuum due to direct nuclear reactions

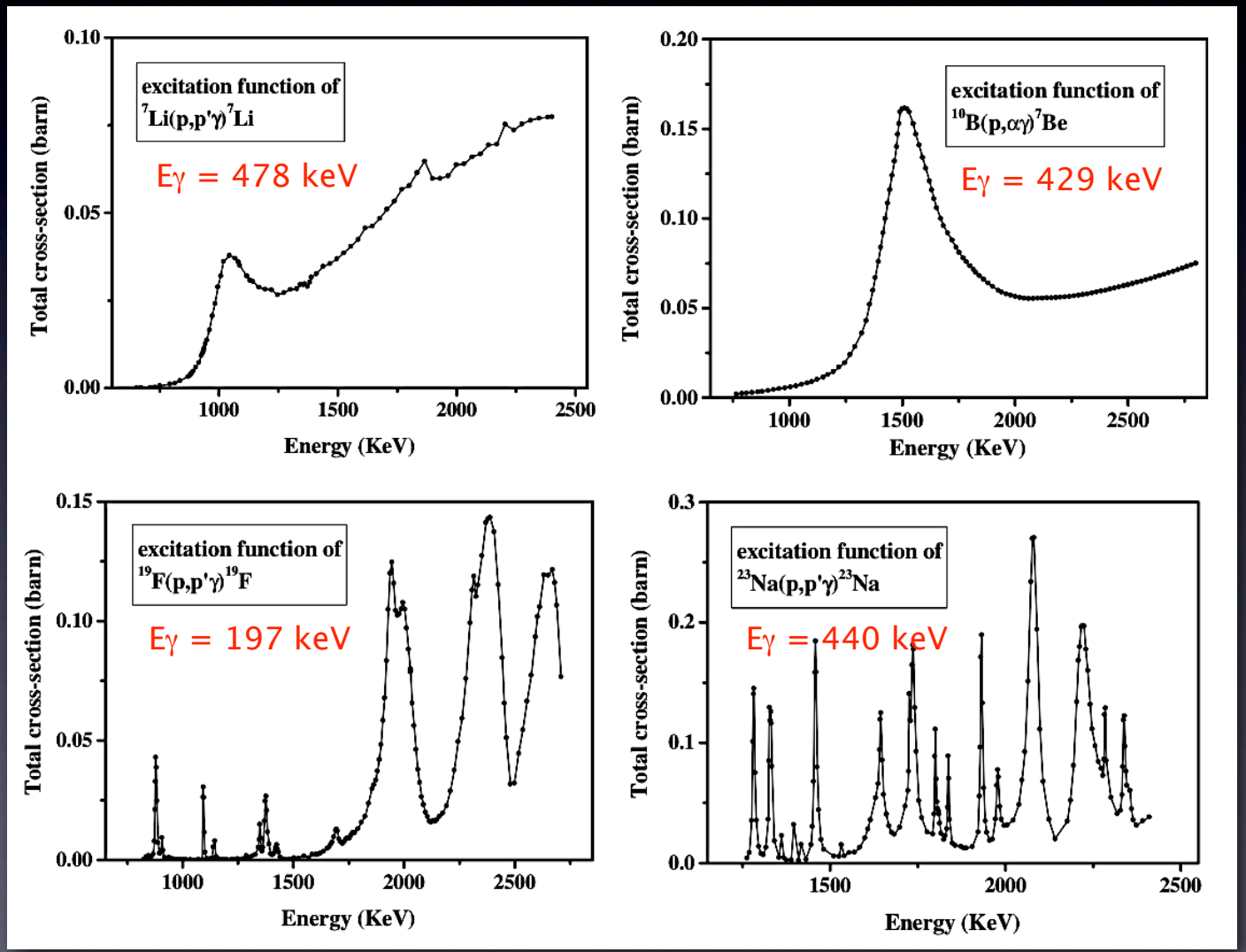

Examples of PIGE spectra

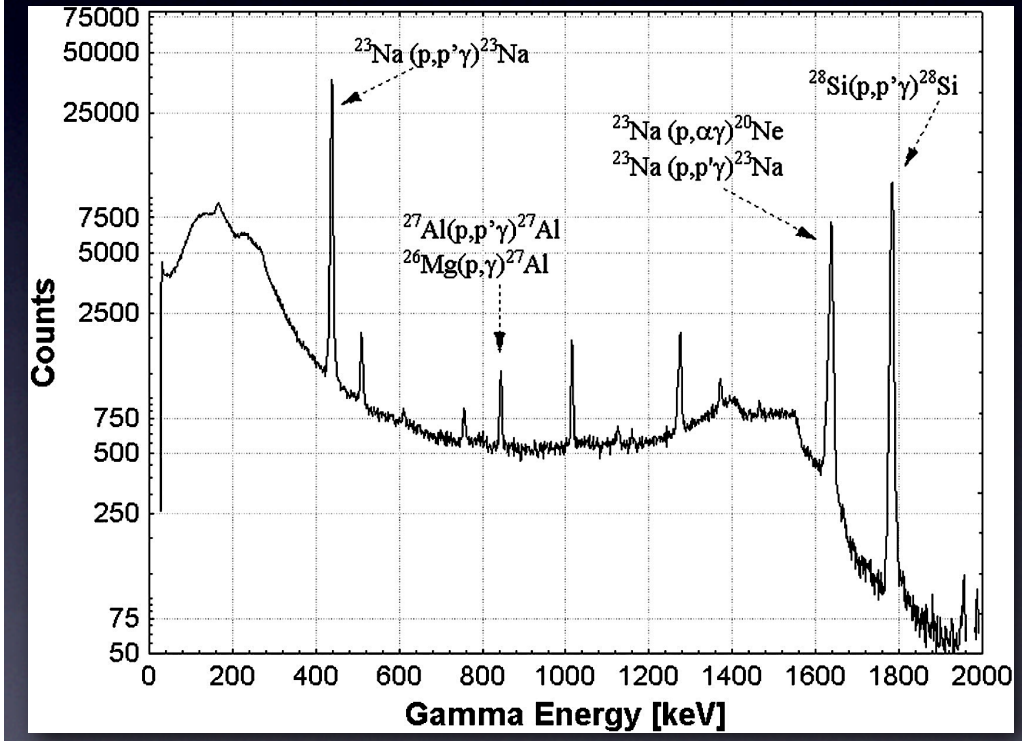

Soda-lime glass

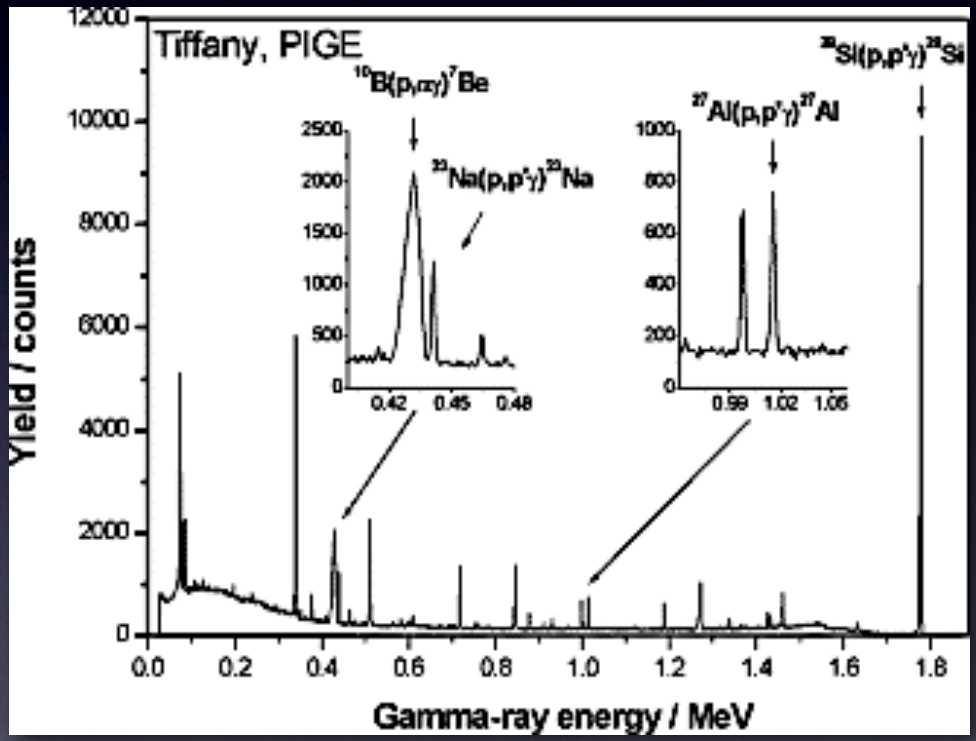

Borosilicate galss

PIGE elemental analysis

The elemental concetrations (N_T) are obtained from measured quantities (i.e. gamma-ray peak areas) using physical models implementing the sample structure and the physical microscopic data and processes:

$$Y_\gamma(E_0,\theta) = \varepsilon_{\text{abs}}(E_\gamma)\cdot N_p \cdot \int_0^{E_0} N_T \cdot \sigma(E_0,\theta)/S(E)\,\mathrm{d}E$$

The principal needed microscopic data are **stopping powers** and **differential cross sections** of the interaction (as well as the detector absolute efficiency)

PIGE analysis in cultural heritage

- The PIGE technique can be used for (semi-)quantitative determination of light elements like Na, Al or Si in infinitely thick targets
- The unknown elemental concentrations are typically deduced by comparing the γ-ray yields with those of **thick** standards of similar composition, without the detailed knowledge of the cross section

Reaction	E γ (keV)
^{23}Na (p, p', γ) ^{23}Na	440
^{25}Mg (p, p', γ) ^{25}Mg	585
^{24}Mg (p, p', γ) ^{24}Mg	1369
^{27}Al (p, p', γ) ^{27}Al	844, 1014
^{28}Si (p, p', γ) ^{28}Si	1779
^{31}P (p, p', γ) ^{31}P	1266

- The crucial point is the difference between the stopping power of the unknown sample and that of the standard

Thick target gamma-ray yields

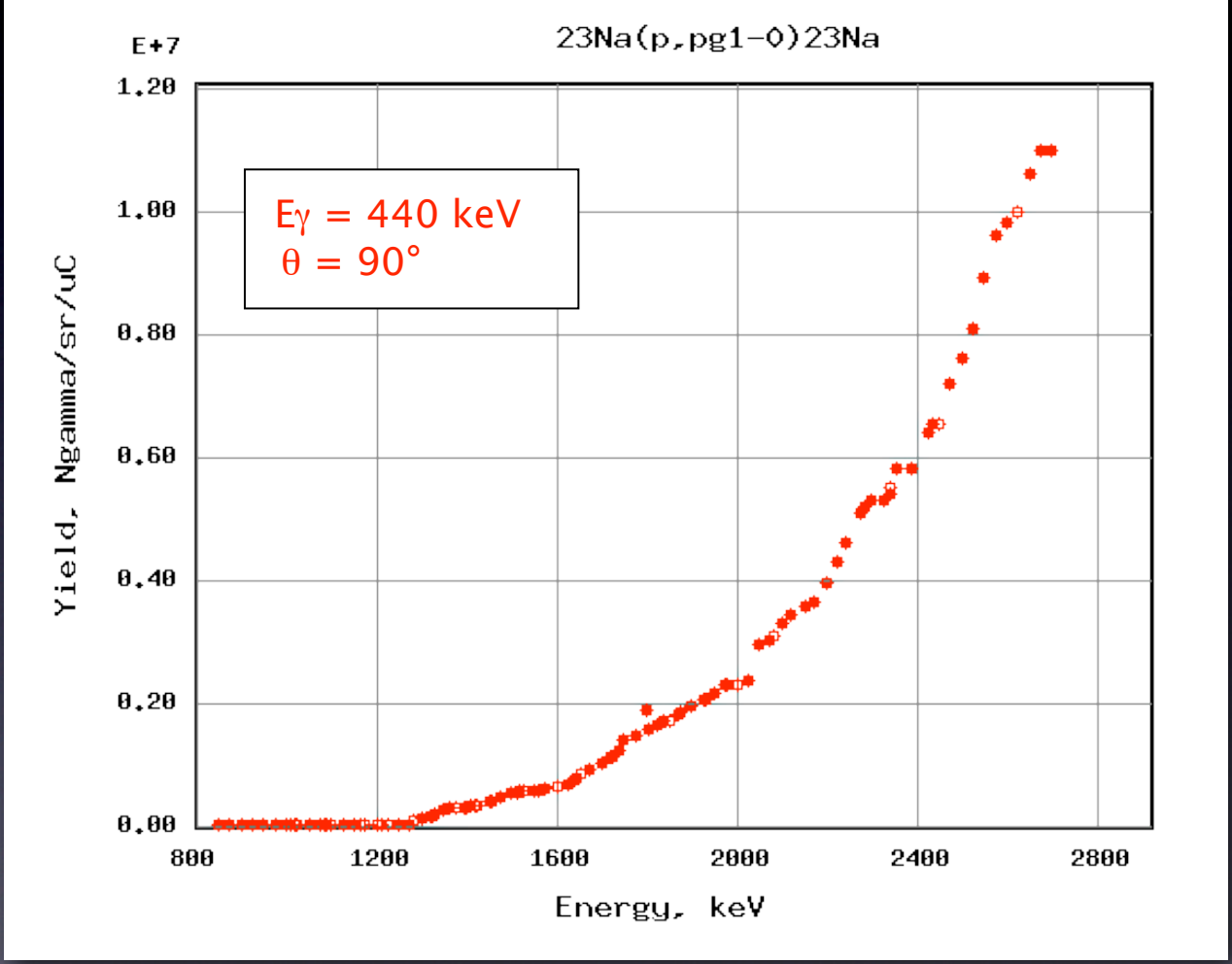

PIGE quantitative analysis: comparison with thick standards

$$C_{camp} = C_{rif} \cdot Y_{camp}(E_0)/Y_{rif}(E_0) \cdot S_{camp}(E_{1/2})/S_{rif}(E_{1/2})$$

$E_{1/2}$ such as:

$$Y(E_0) = 2 \cdot Y(E_{1/2})$$

The "$E_{1/2}$" method is valid as long as the excitation function varies slowly with the energy

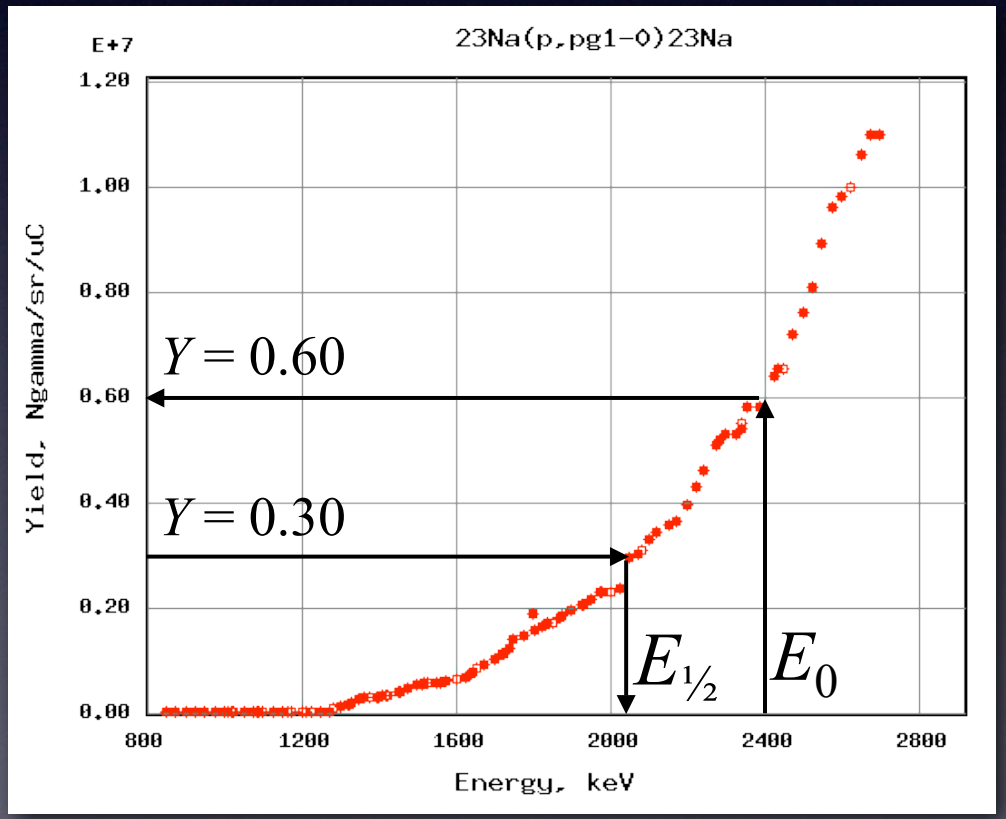

RBS

Rutherford Backscattering Spectrometry

Elastic scattering at backward angles of the impinging ions by the target nuclei

$A > A_p$

✓ depth profile

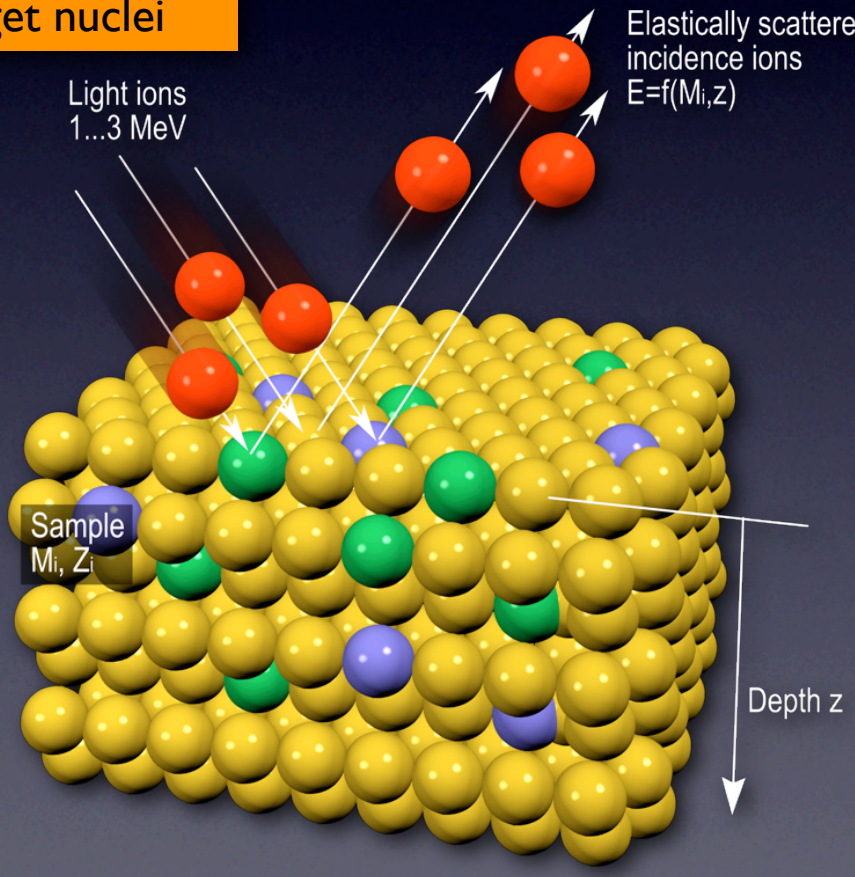

Principles of RBS

For a given scattering angle θ, the energy E_1 of the incident ion (mass M_1) after the collision is only a function of the mass M_2 of the targt nuclei

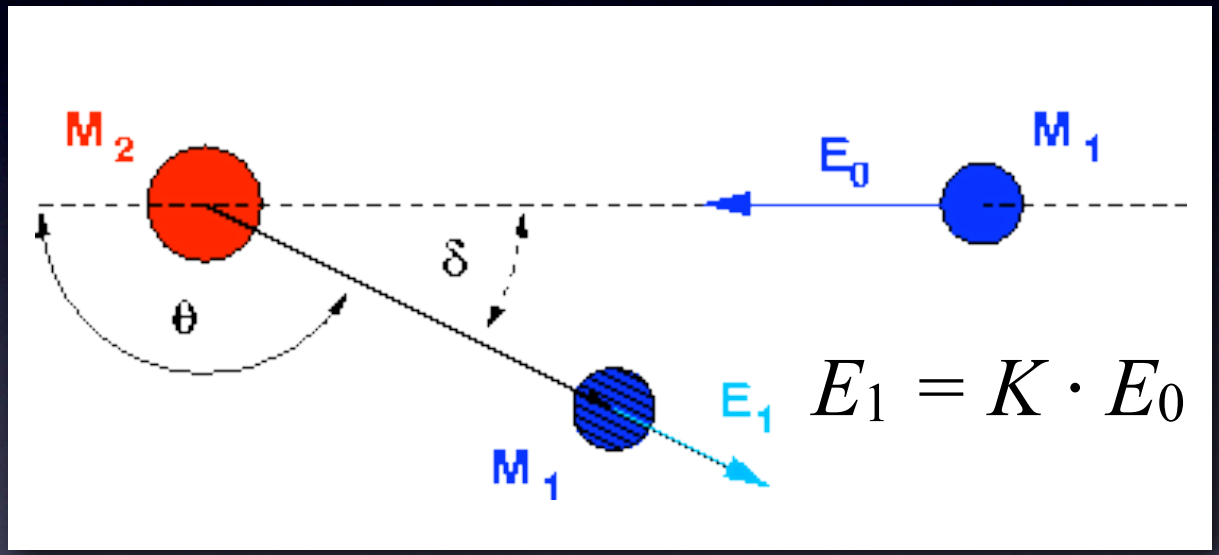

$$K = \frac{\left[\sqrt{\left(\frac{M_2}{M_1}\right)^2 - \sin^2\theta} + \cos\theta\right]^2}{\left(\frac{M_2}{M_1} + 1\right)^2}$$

larger ΔE for smaller M (light nuclei)

Larger ΔE for larger θ (backscattering)

The kinematic factor *K*

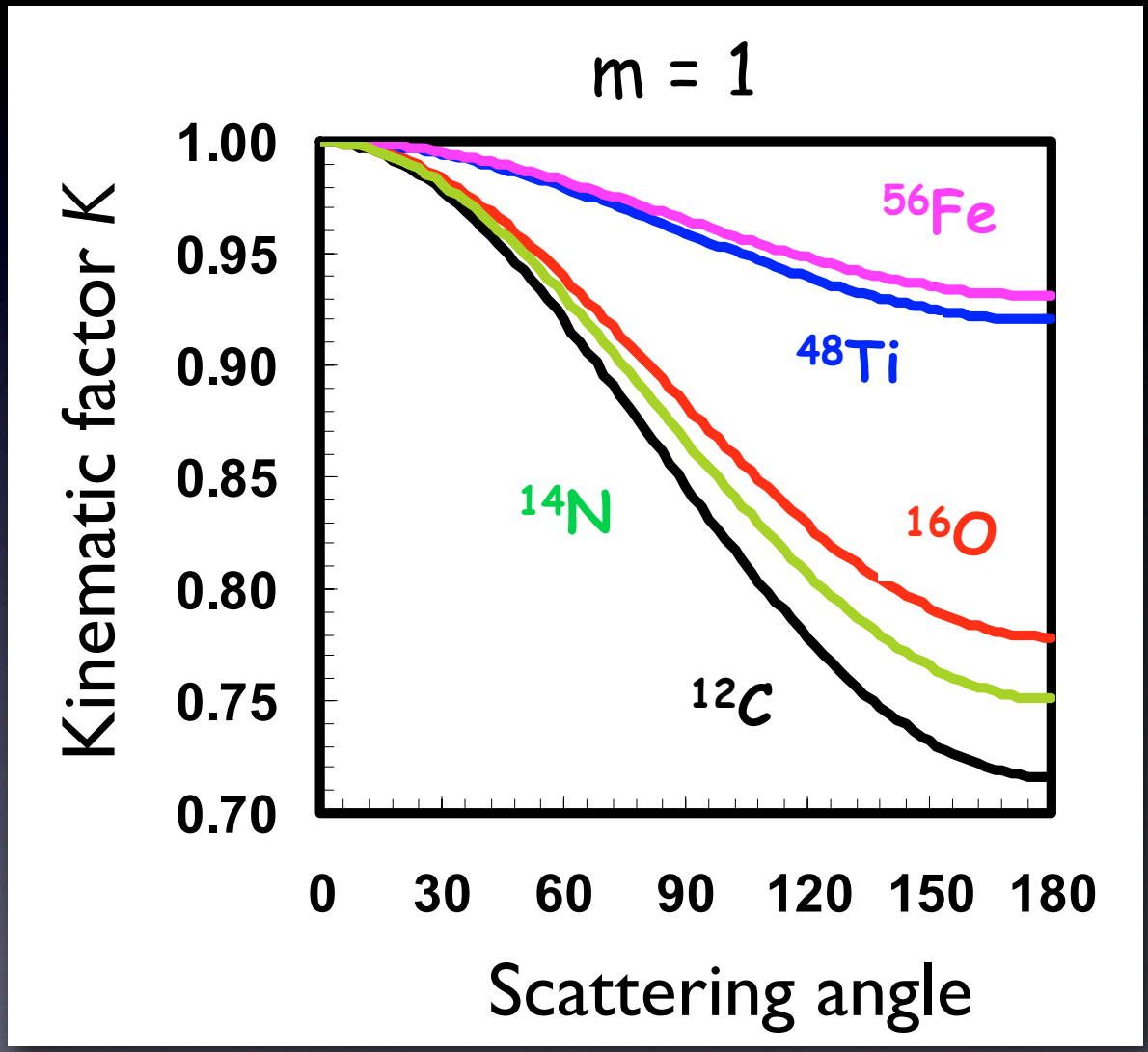

Elastic scattering cross section

The Rutherford formula:

$$\left(\frac{d\sigma}{d\Omega}\right)_{Ruth} = \left(\frac{Z_1 Z_2 e^2}{E}\right)^2 \frac{4}{\sin^4(\theta)} \frac{\left[\sqrt{1-\left(\frac{M_1}{M_2}\sin\theta\right)^2}+\cos\theta\right]^2}{\sqrt{1-\left(\frac{M_1}{M_2}\sin\theta\right)^2}}$$

Z_1 Atomic number of the incident ion

Z_2 Atomic number of the target nucleus

E Energy of the incident ion

M_1 Mass of the incident ion

M_2 Mass of the target nucleus

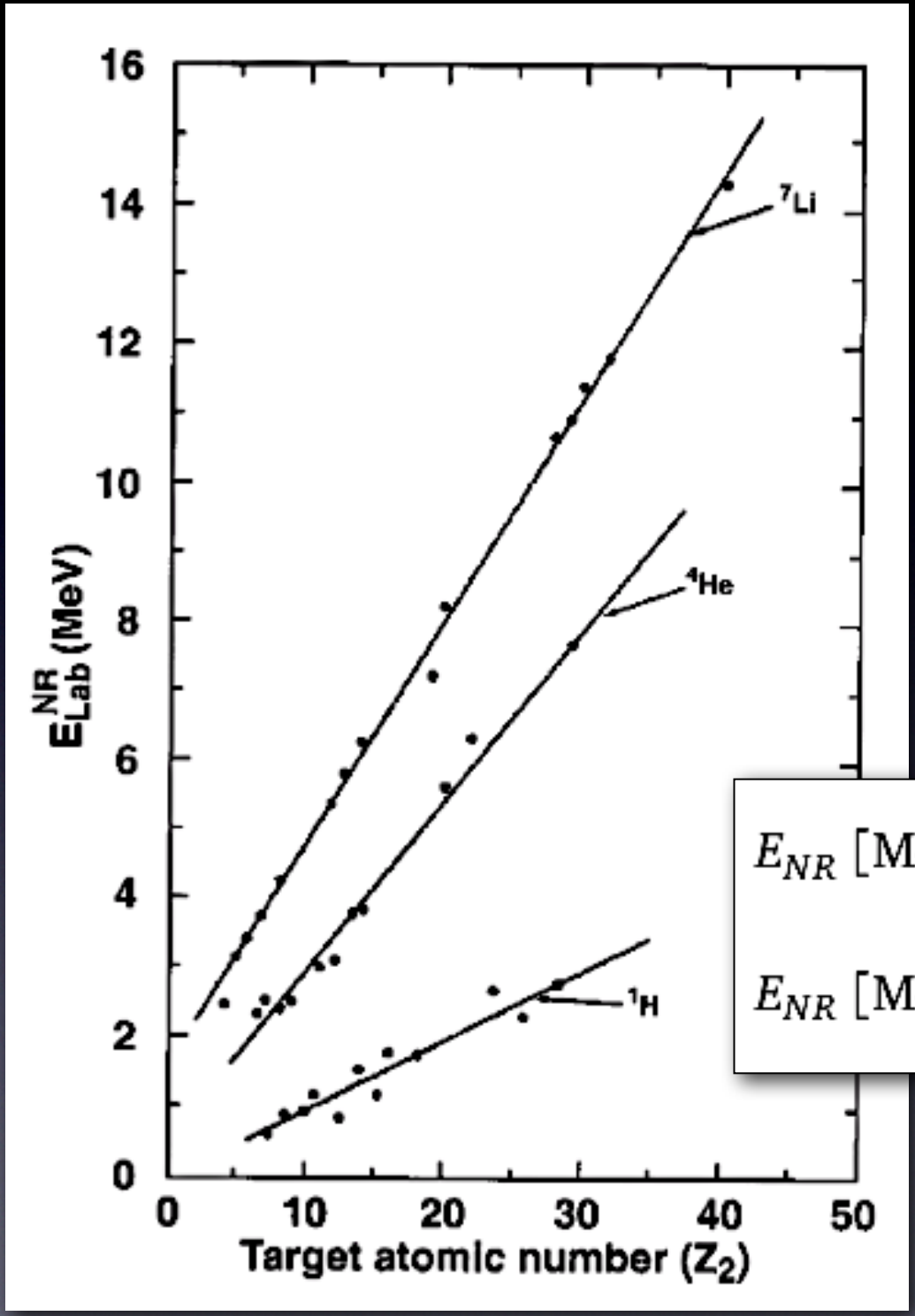

Energy (in the laboratory) at which the elastic scattering cross section deviates more than 4% from the Rutherford value
(for scattering angles > 160°)

$$E_{NR}\,[\mathrm{MeV}] = \frac{M_1 + M_2}{M_2}\frac{Z_2}{10} \quad \text{for } Z_1 = 1$$

$$E_{NR}\,[\mathrm{MeV}] = \frac{M_1 + M_2}{M_2}\frac{Z_1 Z_2}{8} \quad \text{for } Z_1 > 1$$

Non-Rutherford cross sections

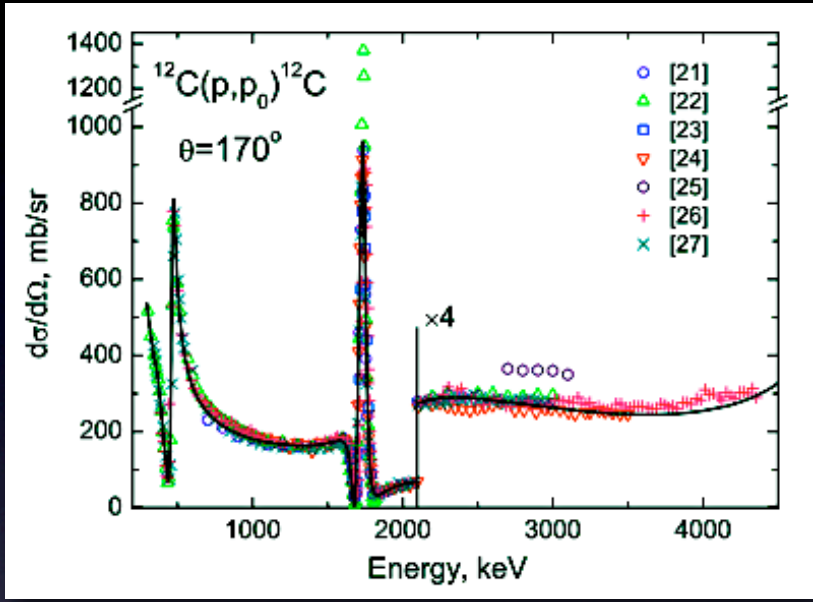

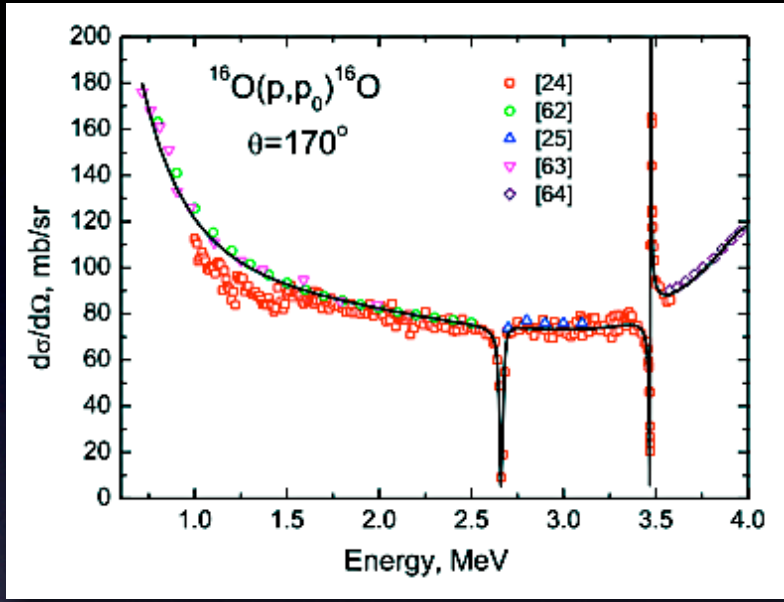

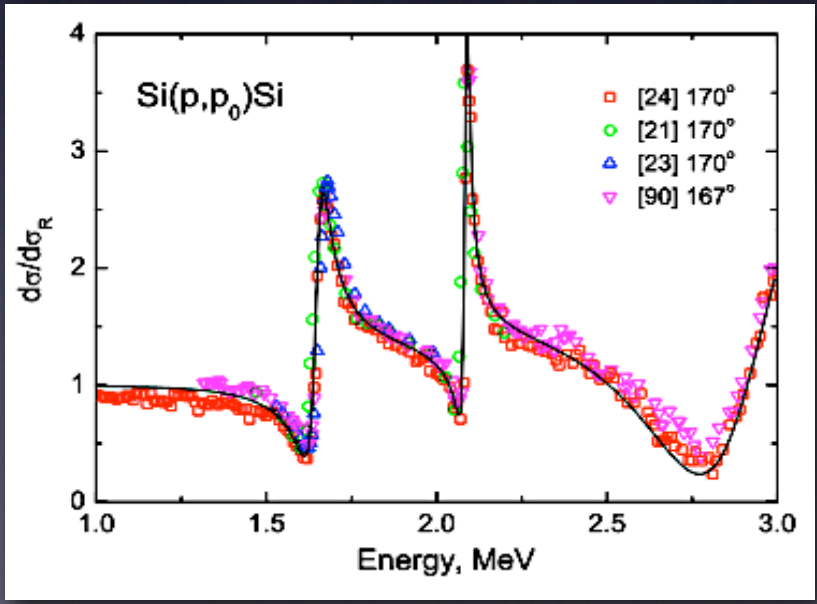

Evaluated and recommended experimental cross sections available from IBANDL web site (www-nds.iaea.org/ibandl/)

Depth scale of RBS

The signal from an atom at the sample surface will appear in the energy spectrum at a position KE_0.

The signal from atoms of the same mass below the sample surface will be shifted by the amount of energy lost while the projectiles pass through the sample, both before (ΔE_{in}) and after a collision (ΔE_{out}).

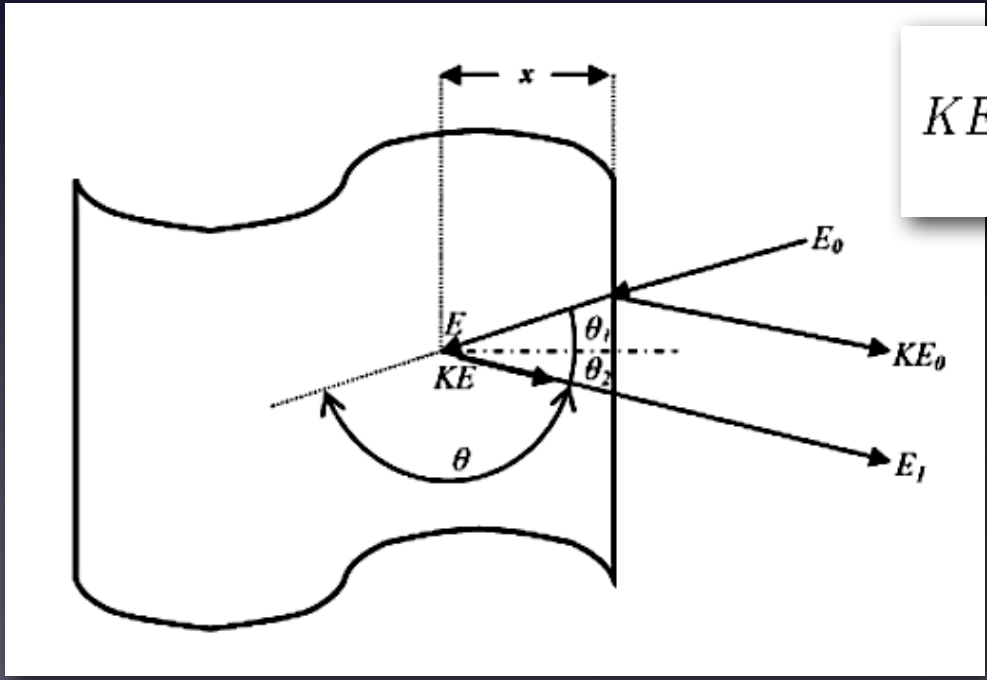

$$KE_0 - E_1 = \left[\frac{Kx}{\cos\theta_1}\cdot\left(\frac{dE}{dx}\right)_{in} + \frac{x}{\cos\theta_2}\cdot\left(\frac{dE}{dx}\right)_{out}\right]$$

There exists a relation between the measured energy E_1 and the depth x at which the scattering took place

The features of RBS spectra

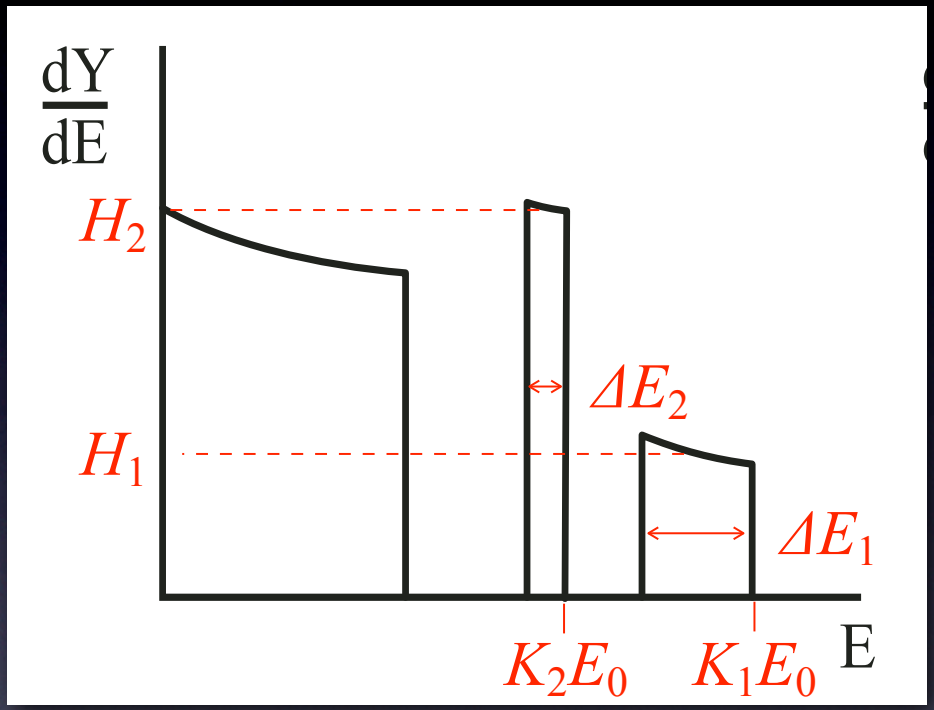

- Position of the signal (mass perception *i.e. kinematic factor*)
- Width of the signal (depth/thickness perception *i.e. stopping force*)
- Heigth of the signal (quantitative analysis of elemental composition *i.e. scattering cross section*)

Examples of RBS spectra

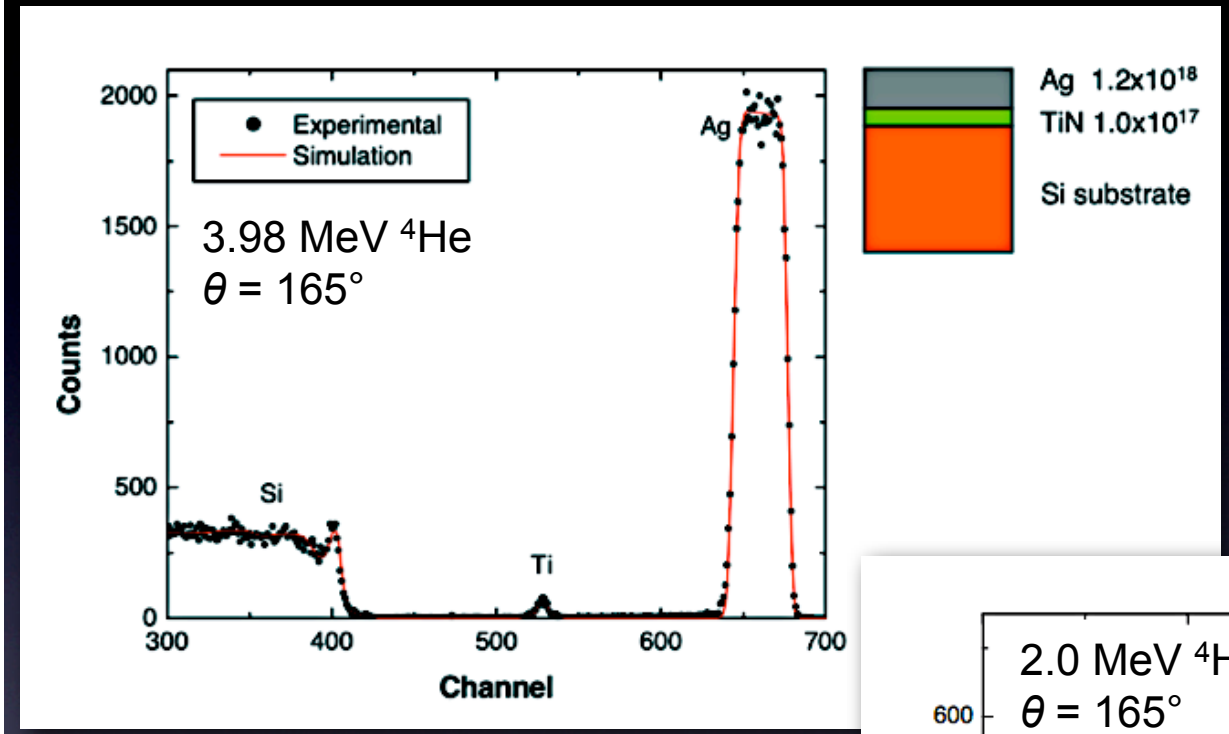

Ag 1.2x10^{18}
TiN 1.0x10^{17}

Si substrate

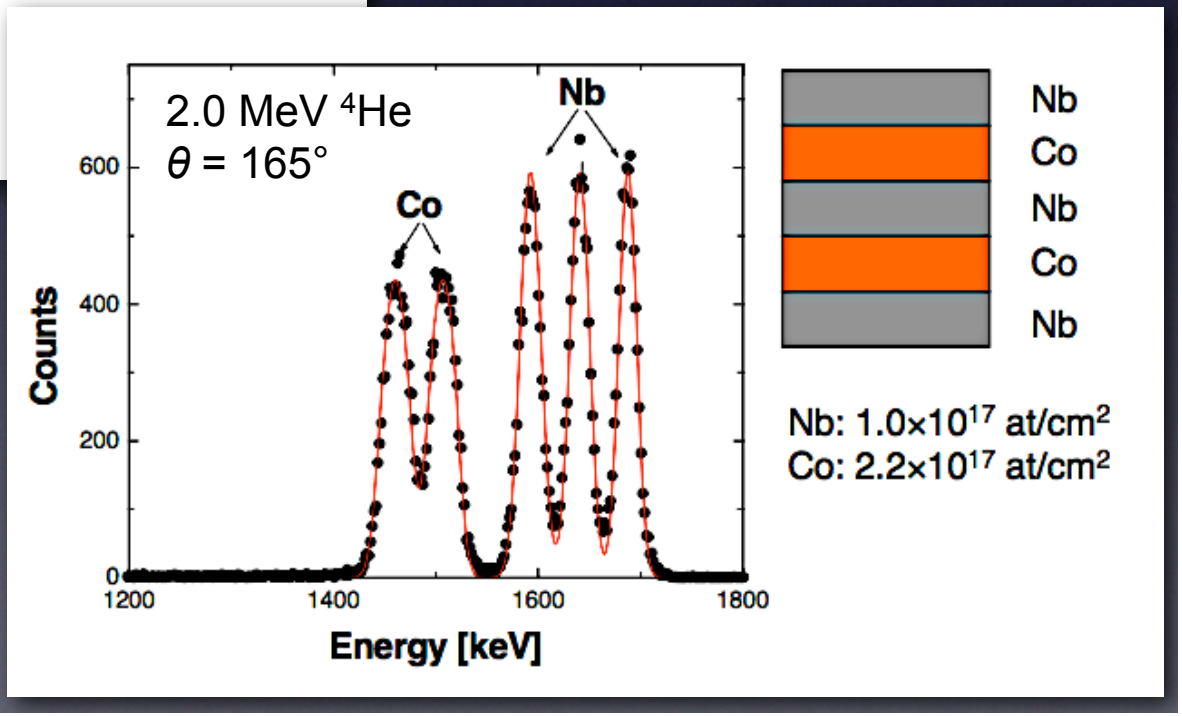

Nb
Co
Nb
Co
Nb

Nb: 1.0×10^{17} at/cm^2
Co: 2.2×10^{17} at/cm^2


Do extracted ion beams look like these?

External beam

Advantages

- direct analysis of artefacts having any shape and any size
- no sampling
- no charging, no preparation (conductive coating etc.)
- no heating, reduced damage risk
- easy sample positioning
- fast and efficient

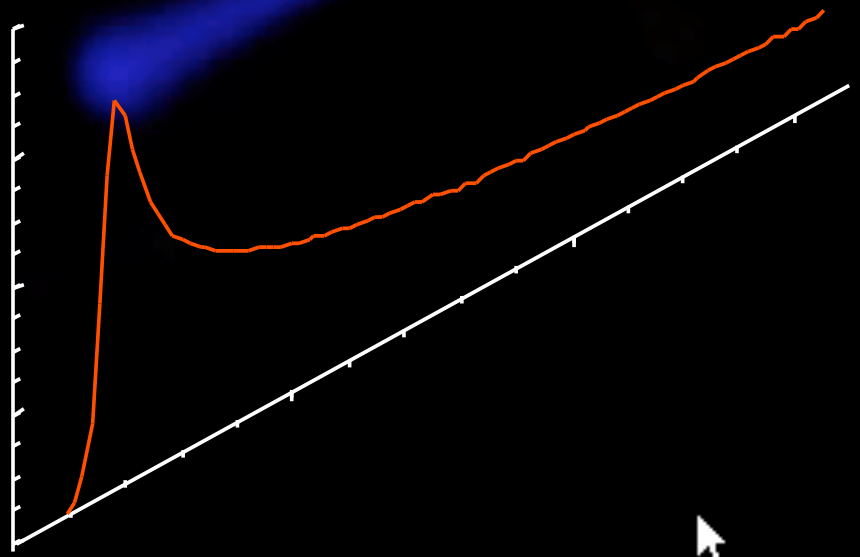

Disadvantages

- energy loss
- energy straggling
- beam lateral spread
- x-ray attenuation

Typical extraction windows

Material	Thickness (μm)	ΔE (keV)	σ_E (keV)	σ_θ (μm/mm)
Al	10	235	16	14
Kapton	8	130	9	6
Zr	2	75	7.3	15
Si_3N_4	0.1	8	5	<1
	0.5	40	9	<2

Choice of external atmosphere

Air

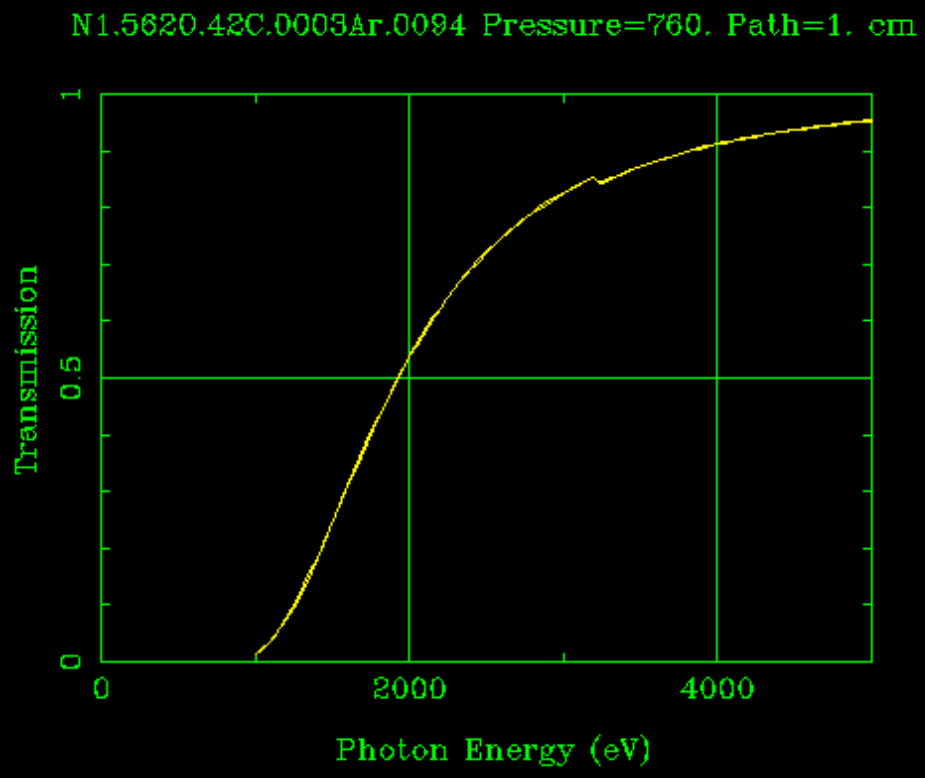

Helium

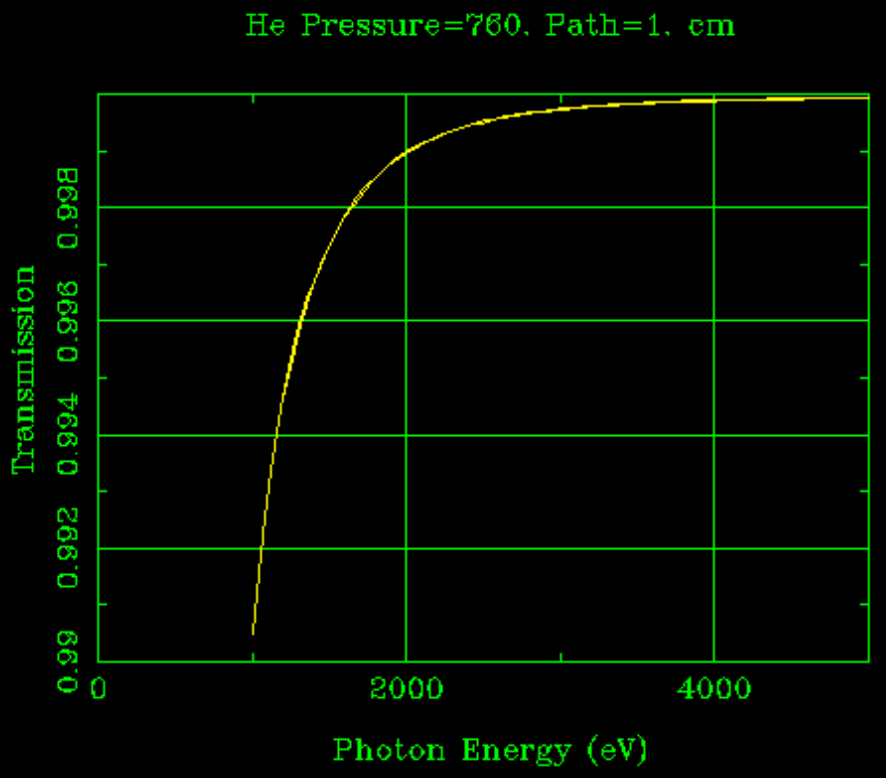

The use of an helium-saturated atmosphere in front of the X-ray detector is mandatory

External beam IBA of ancient manuscripts, ...ceramics,

PIXE analysis of the frontispiece of Pl.16,22, from Biblioteca Laurenziana in Florence

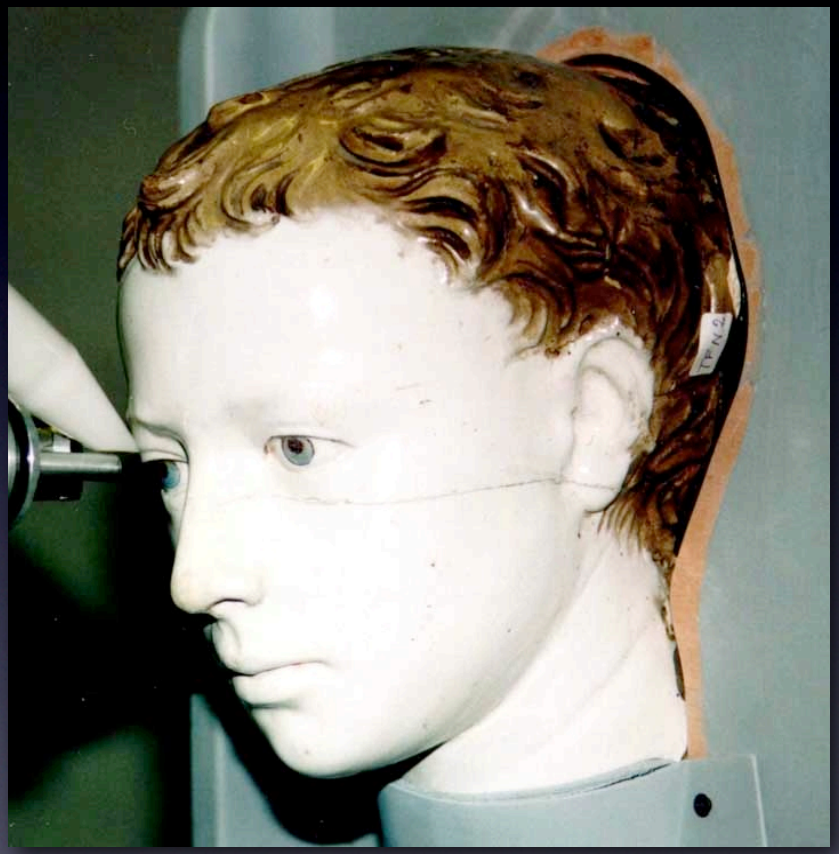

Analysis of the Ritratto di fanciullo by Luca Della Robbia – before restoration at the Opificio delle Pietre Dure in Florence

… drawings,

Micro-PIXE measurements of Portrait of Lucas de Leyde by Alfred Dürer

A.Duval et al., (Louvre laboratory)

... jewels,

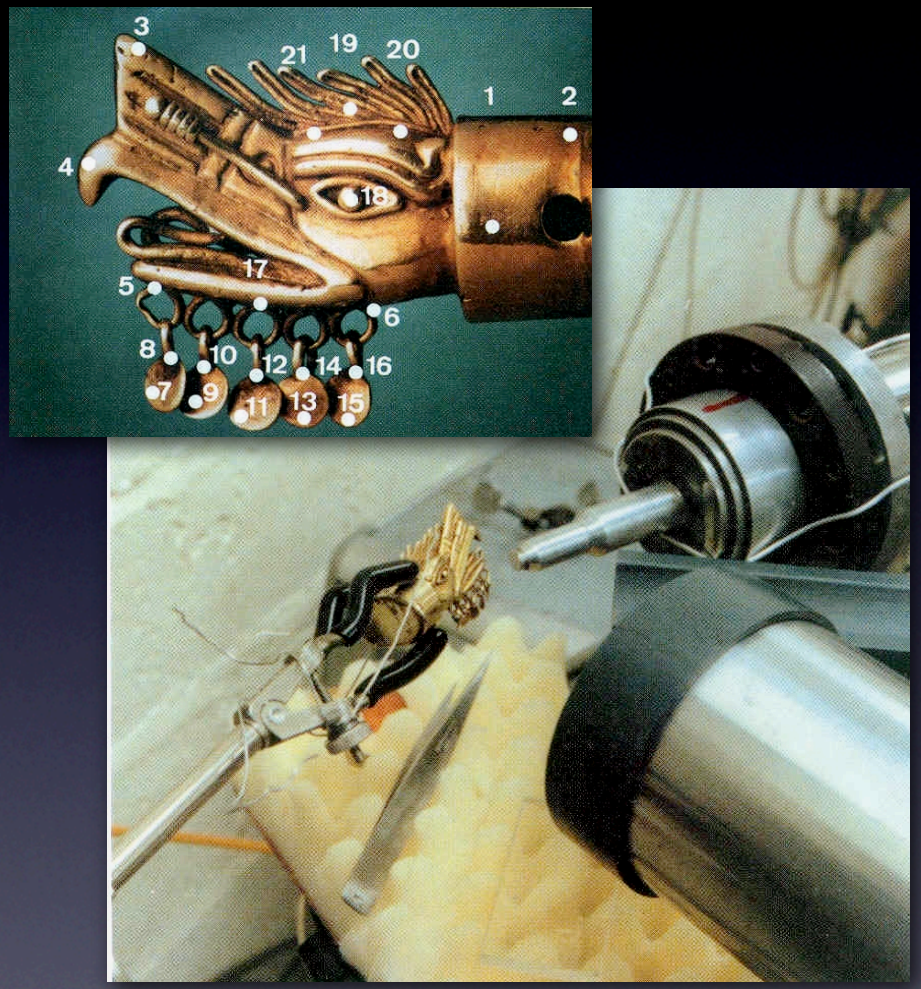

Micro-PIXE measurements of a Mexican gold alloy ornament

G.Demortier and J.L.Ruvalcaba Sil (Namur)

...paintings

PIXE analysis of a painting by
Lucas Cranach the Elder
C. Neelmeijer et al.
(Rossendorf Forschungszentrum, Dresda)

Blue Temperas

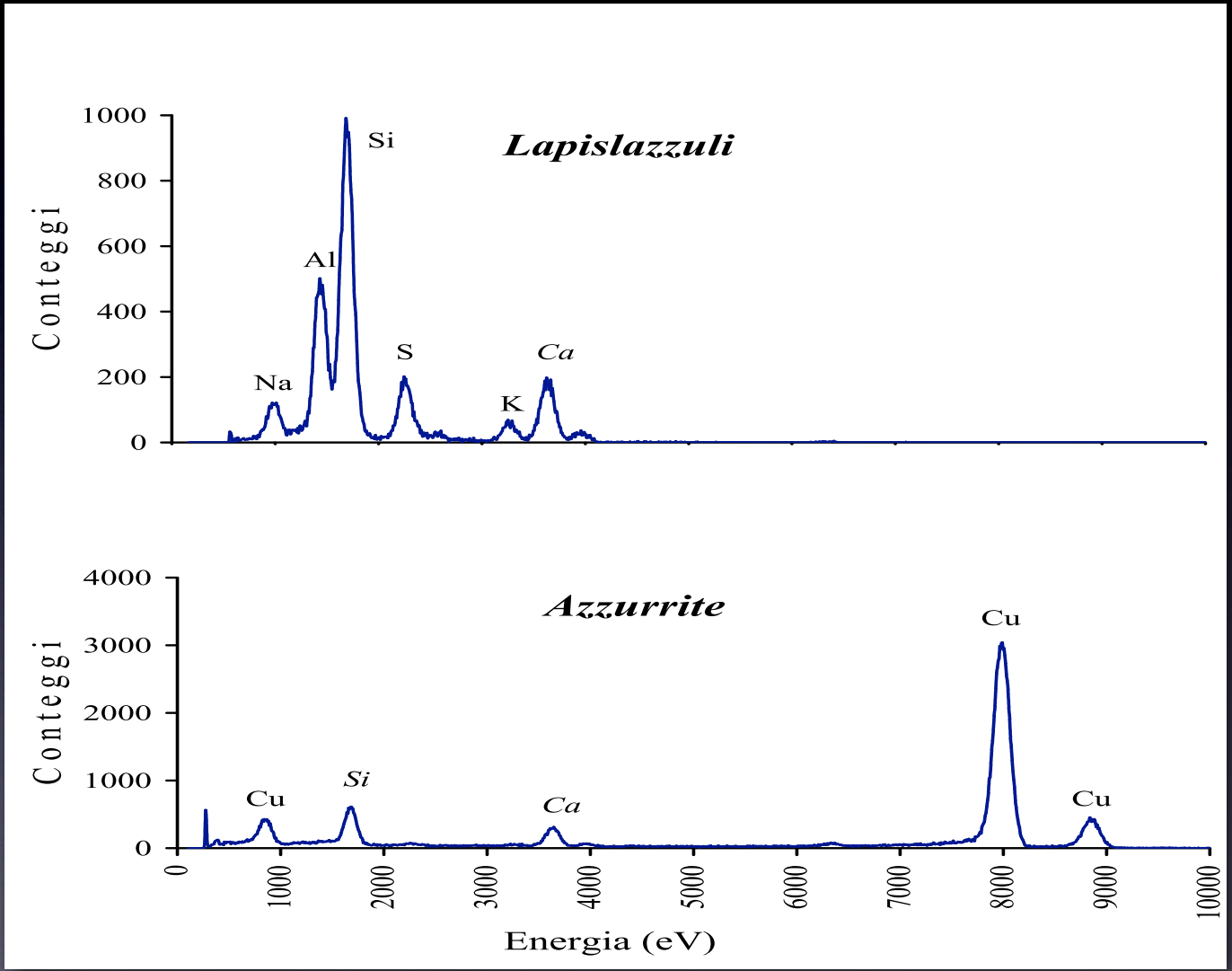

Example of PIXE spectra of two blue pigments

Blue Temperas

Pluteo 48, 34, f. 66 v°

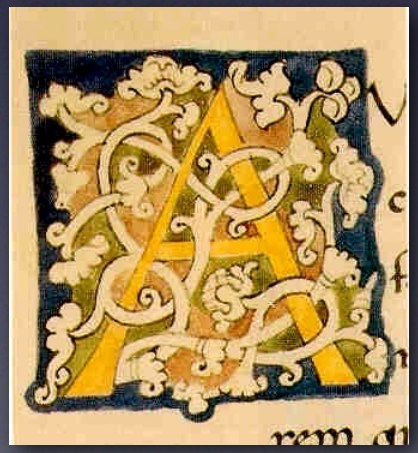

Pluteo 48, 34, f. 41 v°

Extensive use of lapislazuli starting from XI century

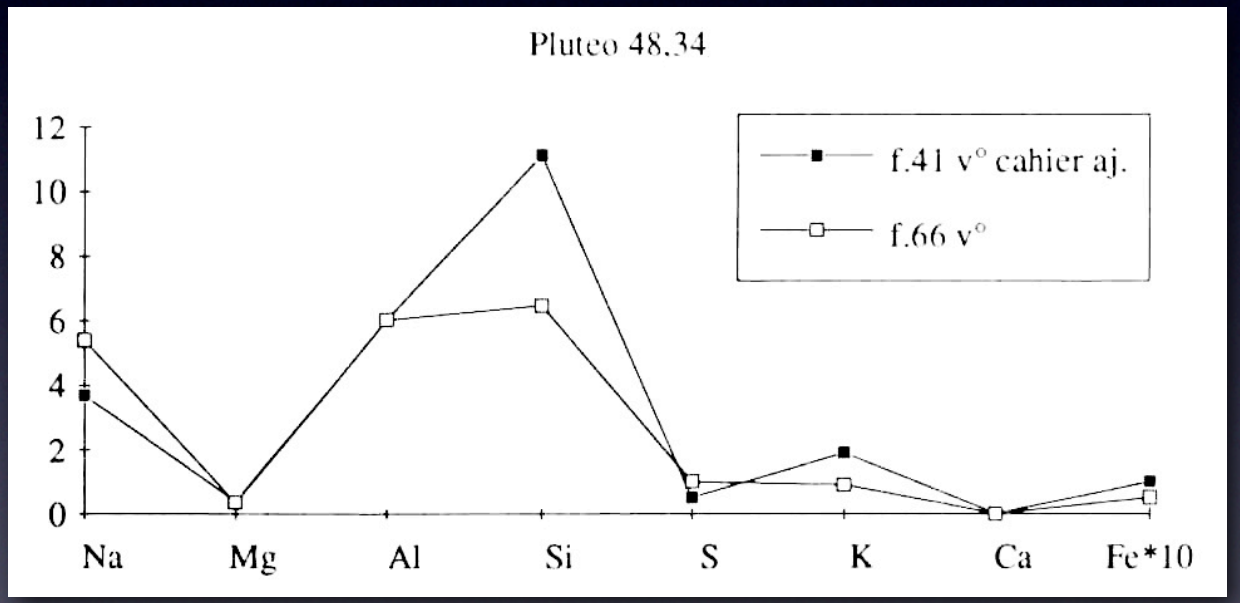

Metal point drawings

LEONARDO DA VINCI
STUDY OF A DRAPERY
Roma, Istituto Nazionale per la Grafica

metal point, lead white
red prepared paper

Characteristics of metal point drawings

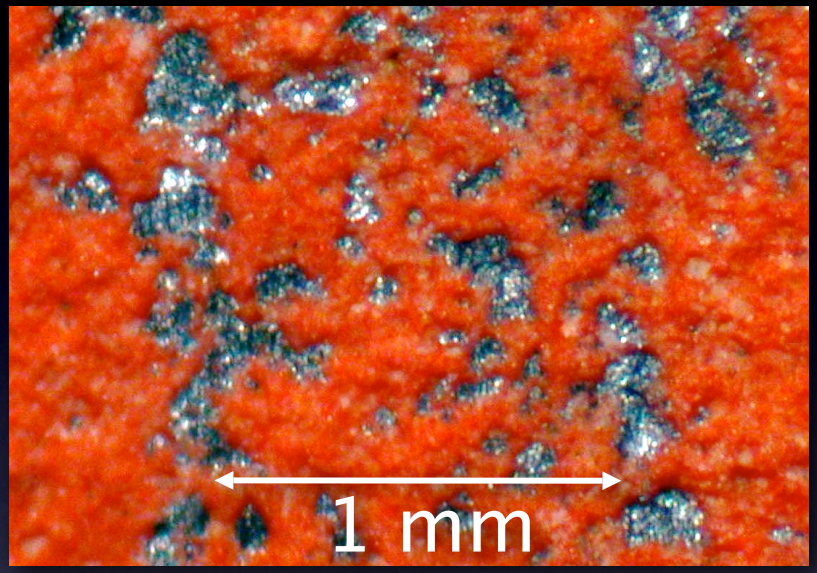

The extension of the metallic agglomerates on the surface is some tens of μm

The beam size does not allow a detailed analysis

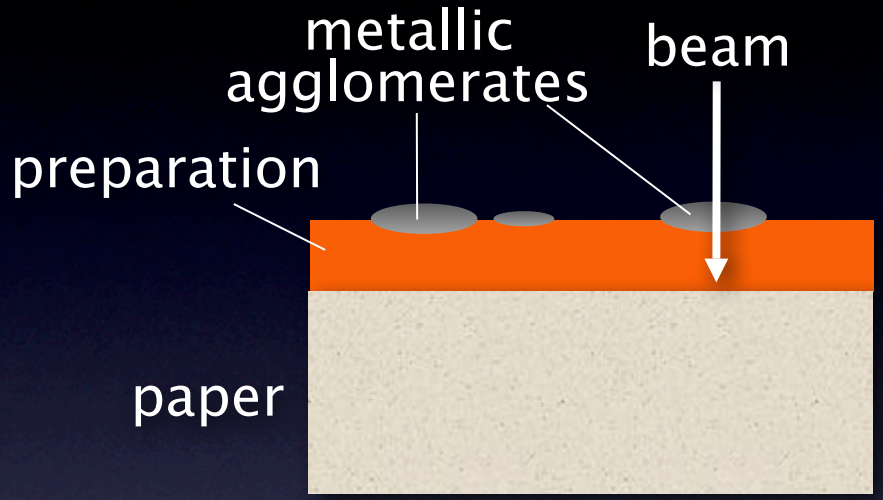

The beam can pass through the trace and hit the preaparation

The contribution of the preparation must be taken into account

Nuclear microscopy

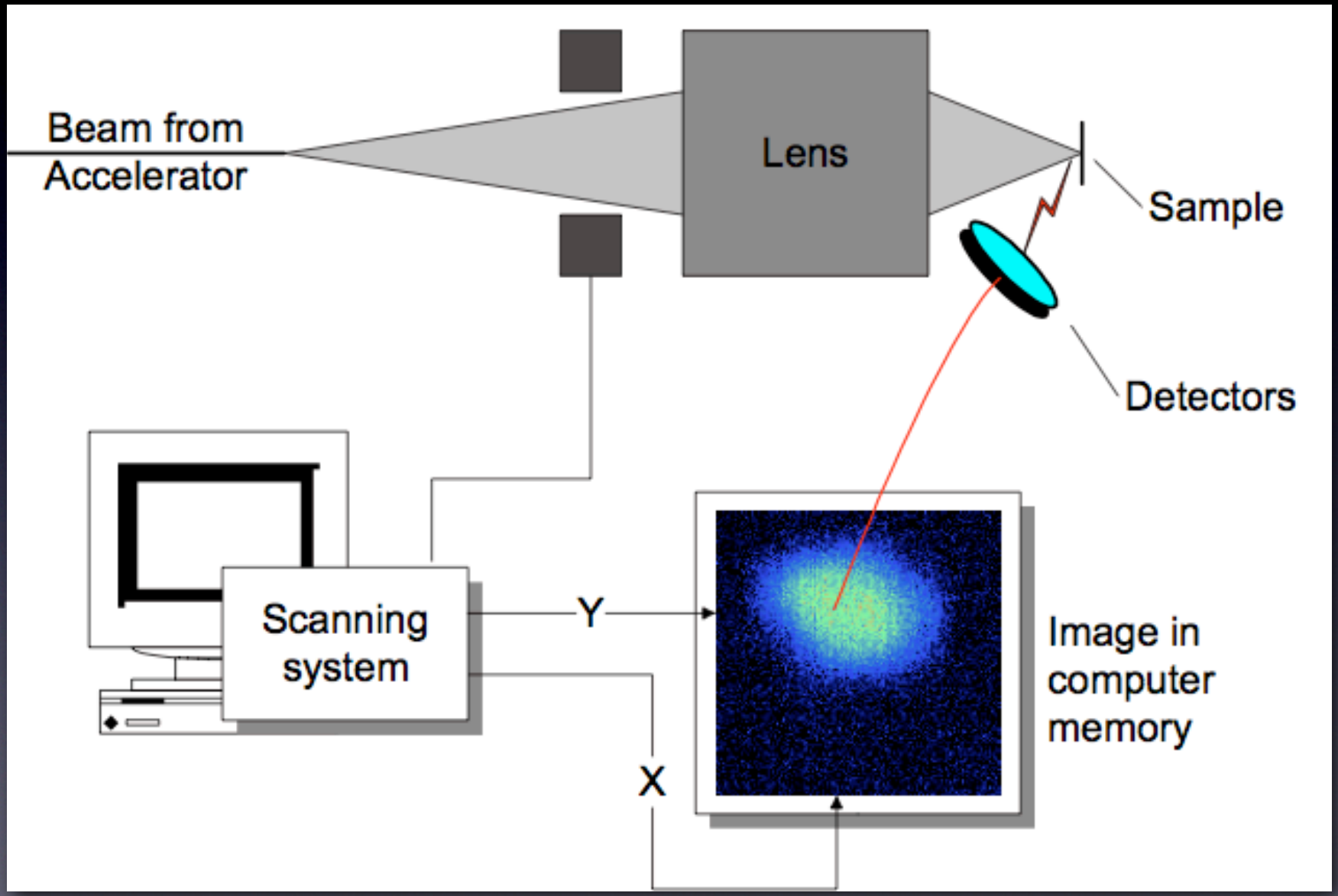

MicroPIXE analysis of metal point drawings

Four metallic points:
silver, lead, gold, copper

Red preparation:
cinnaber, yellow ochre,
lead white, bone white

Au Cu Pb

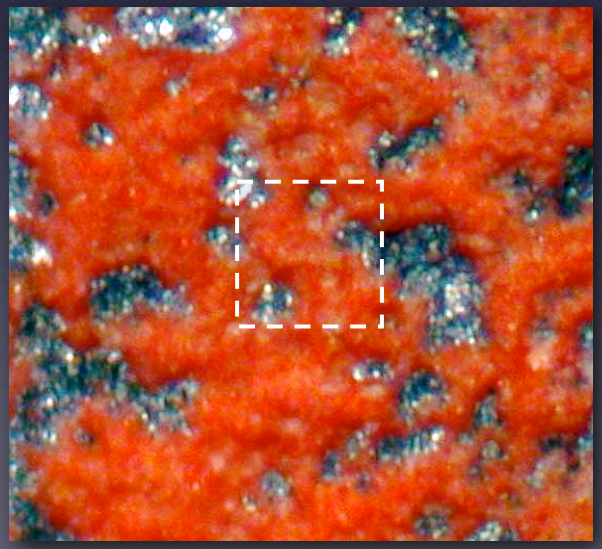

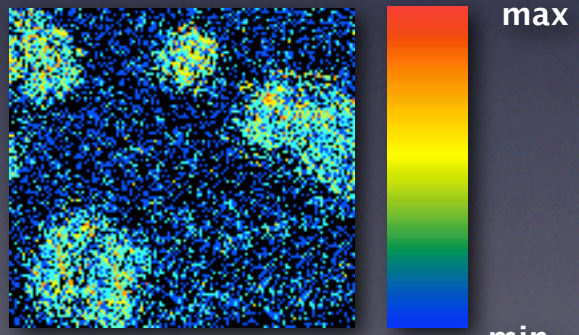

Elemental map on
0.4×0.4 mm²

Lead stylus
(**Pb**, trace of Sn)

Red preparation
(S, Hg, Pb, Fe, P, Ca)

Micro-PIXE measurements of an Achemenide pendant (IV century BC)

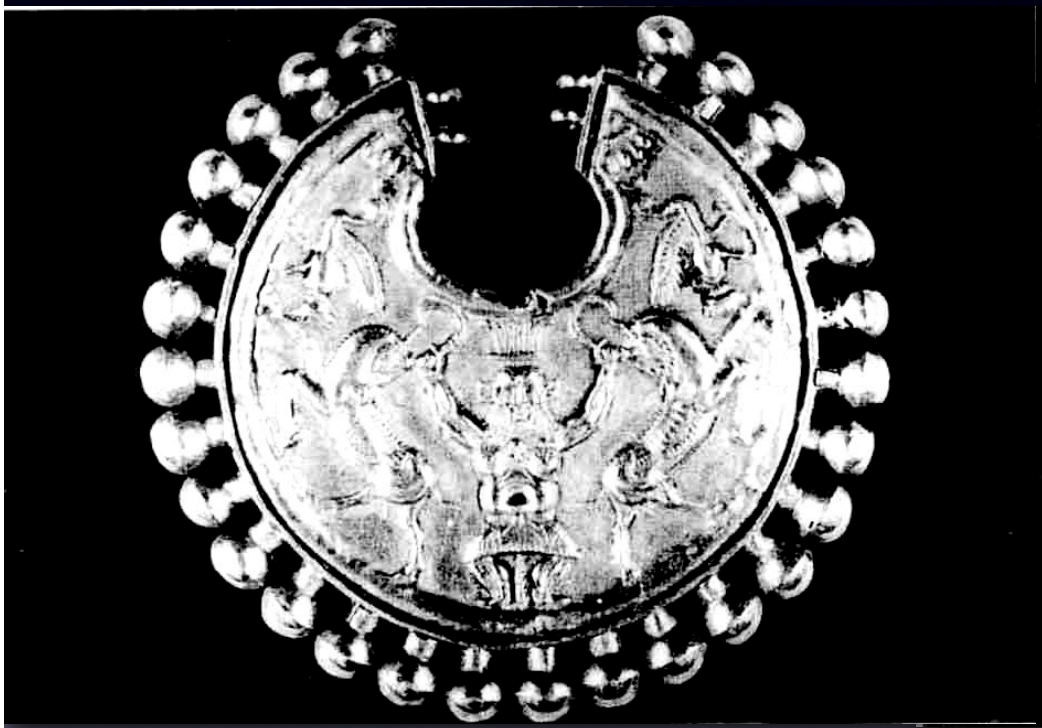

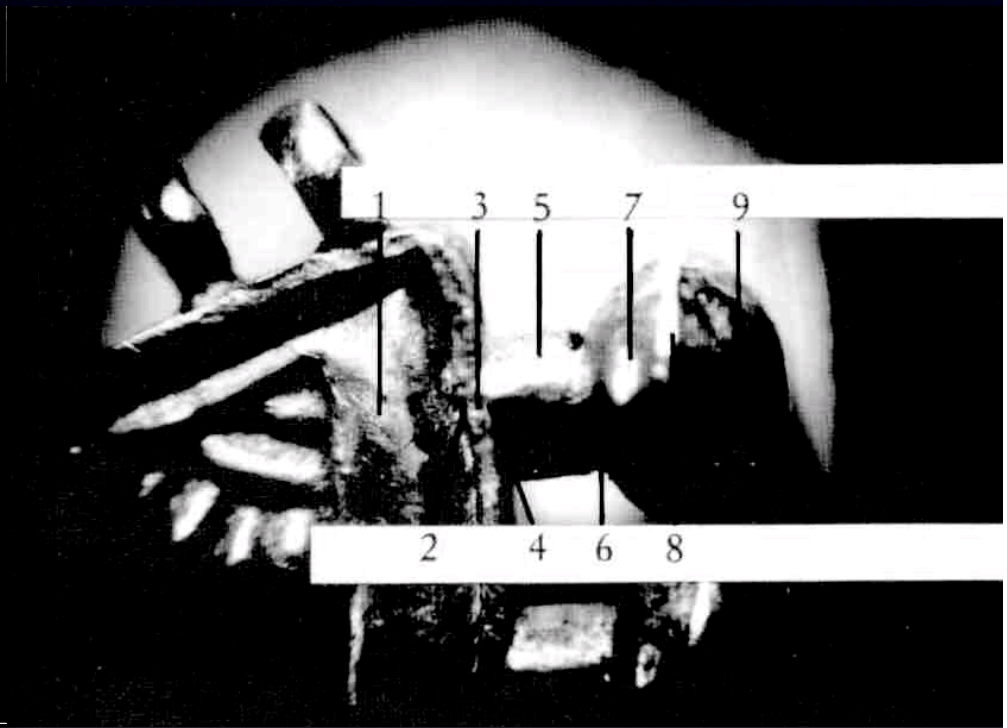

Micro-PIXE measurements of an Achemenide pendant (IV century BC)

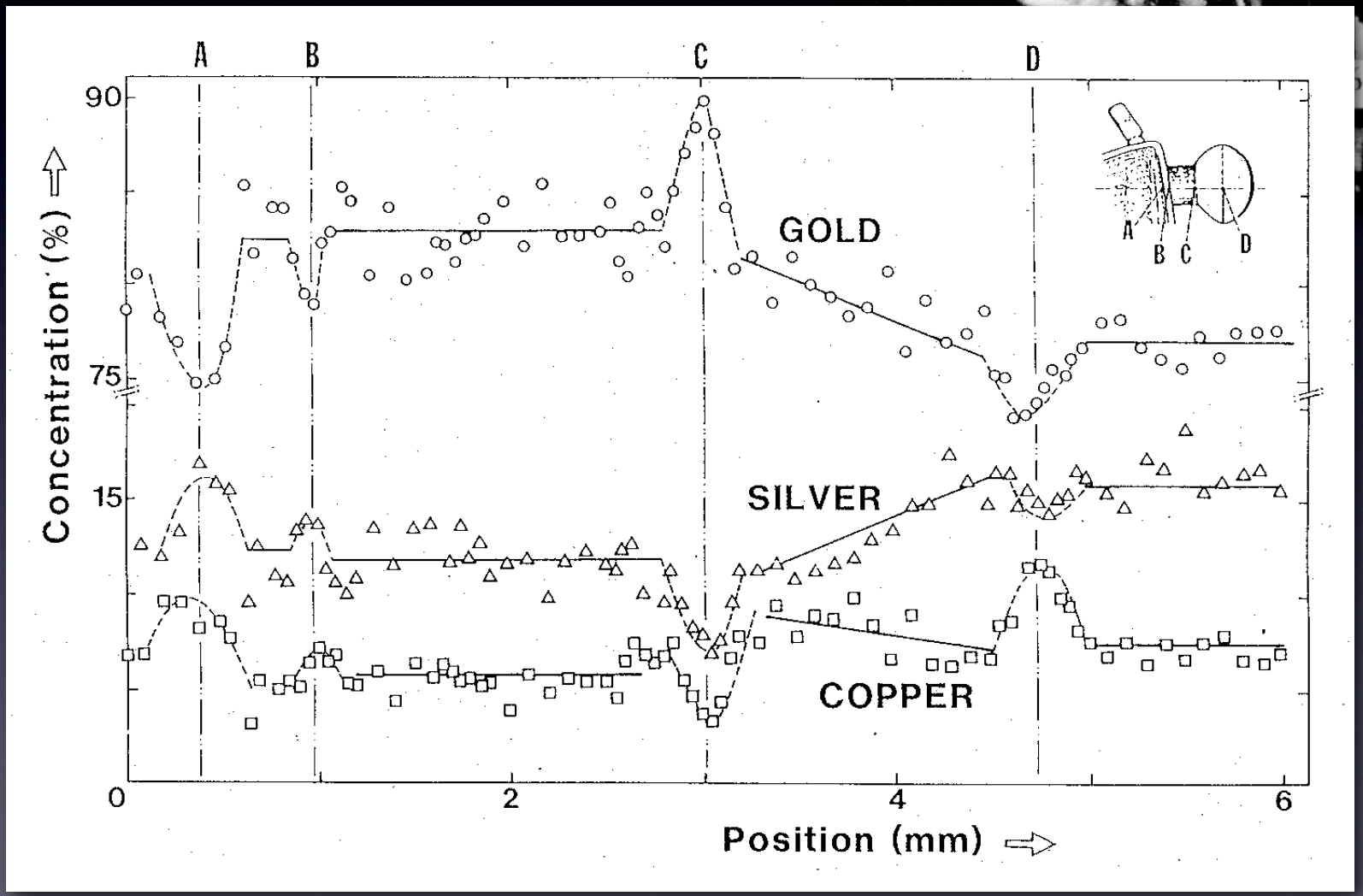

Differential PIXE

Consists in performing measurements on the same area with beams of different energies

At different energies proton beam ranges are different

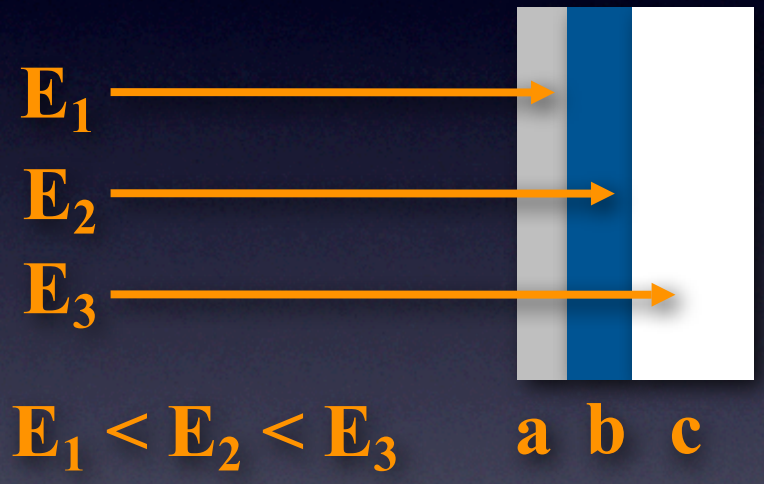

By comparing X-ray spectra taken at different energies, stratigraphic information can be obtained

PIXE spectra at different energies

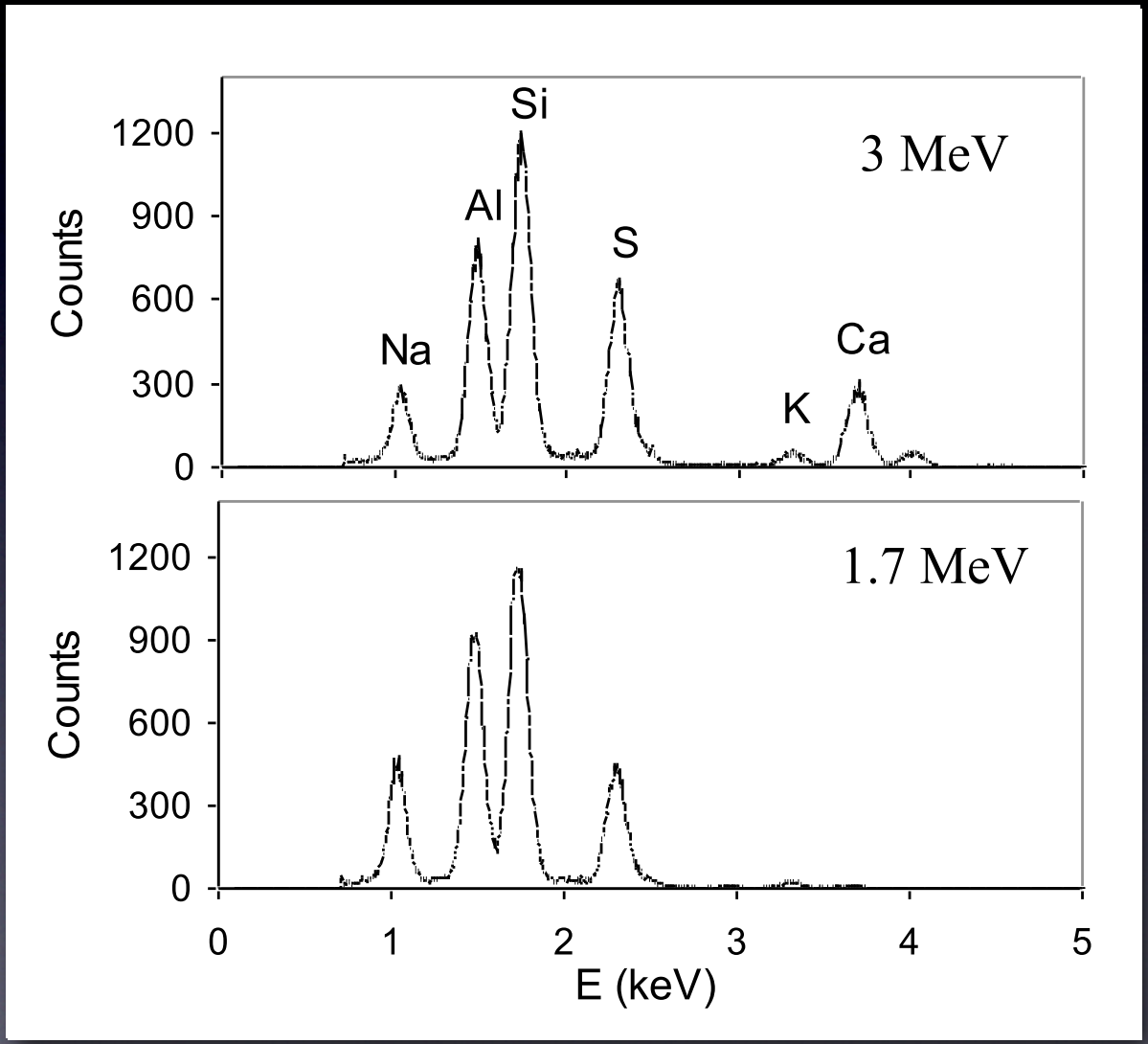

Blue paint layer (lapislazuli) on a substrate of calcium sulphate

Estimate of the paint layer thickness

$$\frac{Y_{\mathrm{Al}}}{Y_{\mathrm{Ca}}} = \frac{C_{\mathrm{Al}}}{C_{\mathrm{Ca}}} \frac{\int_{E_\mathrm{p}}^{E_\mathrm{p}-\Delta E_{\mathrm{lap}}(t)} \sigma_{\mathrm{X}}^{(\mathrm{Al})}(E) \mathrm{e}^{-\mu_{\mathrm{lap}}^{(\mathrm{Al})} \frac{x(E)}{\cos\theta}} \frac{\mathrm{d}E}{S_{\mathrm{lap}}(E)}}{\mathrm{e}^{-\mu_{\mathrm{lap}}^{(\mathrm{Ca})} \frac{t}{\cos\theta}} \int_{E_\mathrm{p}-\Delta E_{\mathrm{lap}}(t)}^{0} \sigma_{\mathrm{X}}^{(\mathrm{Ca})}(E) \mathrm{e}^{-\mu_{\mathrm{white}}^{(\mathrm{Ca})} \frac{x'(E)}{\cos\theta}} \frac{\mathrm{d}E}{S_{\mathrm{white}}(E)}}$$

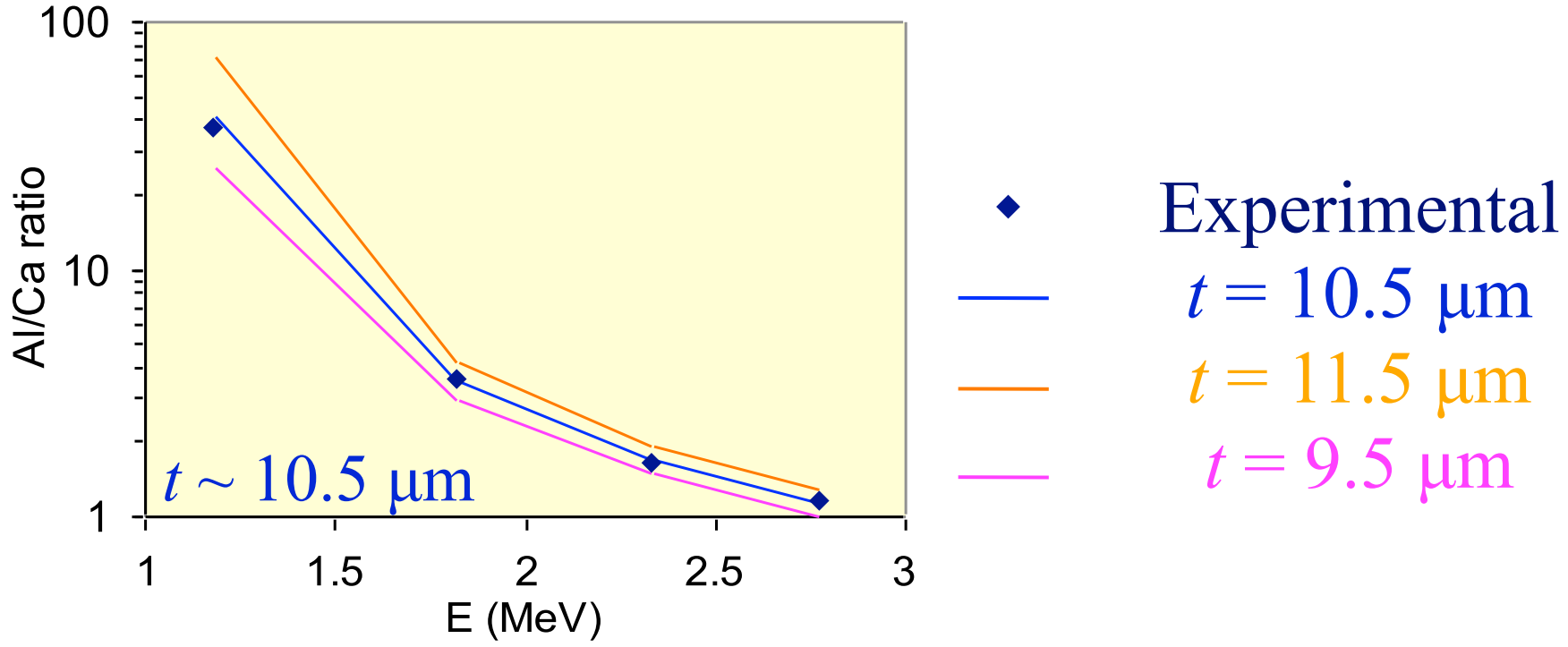

Metal threads (Alhambra, Granada)

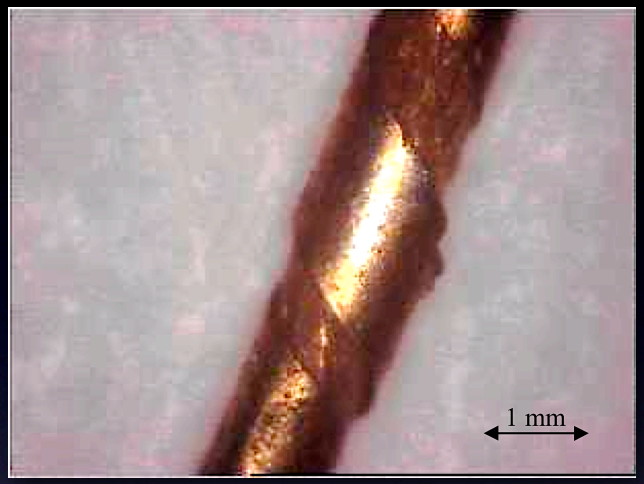

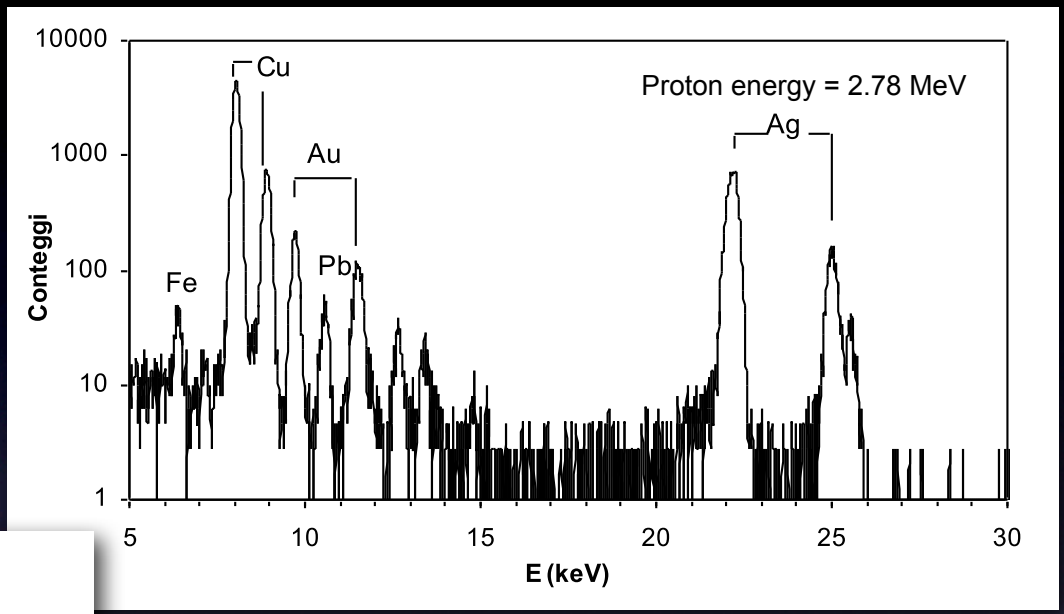

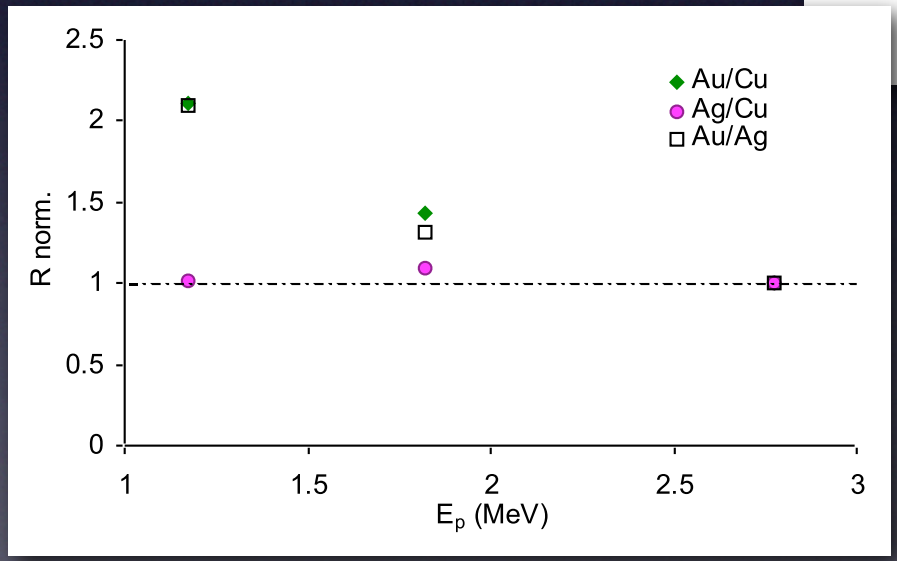

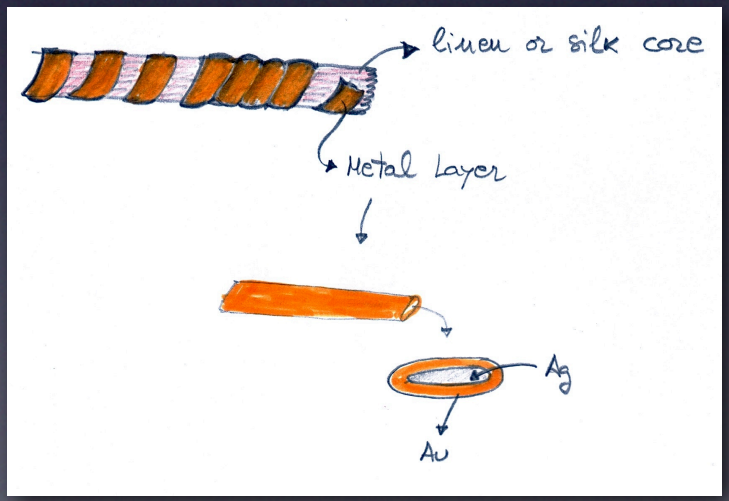

Enrichment of gold on the surface

“Incarnato”

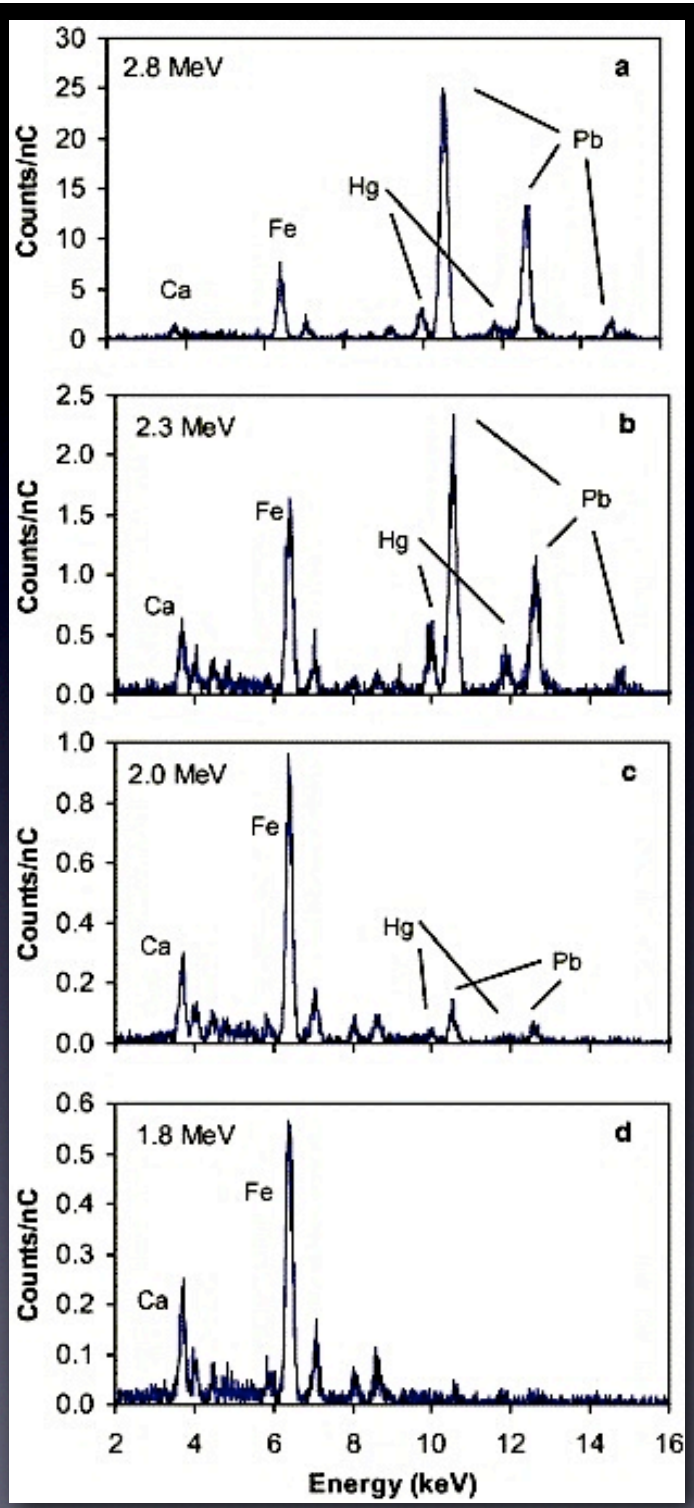

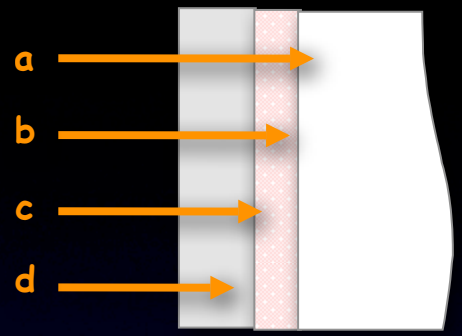

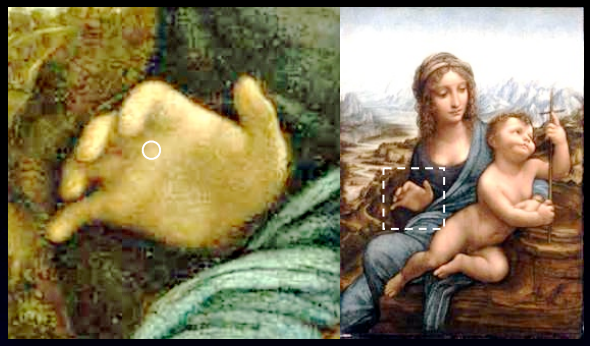

paint layer:

cinnabar (HgS, red pigment)+lead white

preparation:

lead white

Ca and Fe are in the varnish

Lapis-lazuli pigment in paint layers

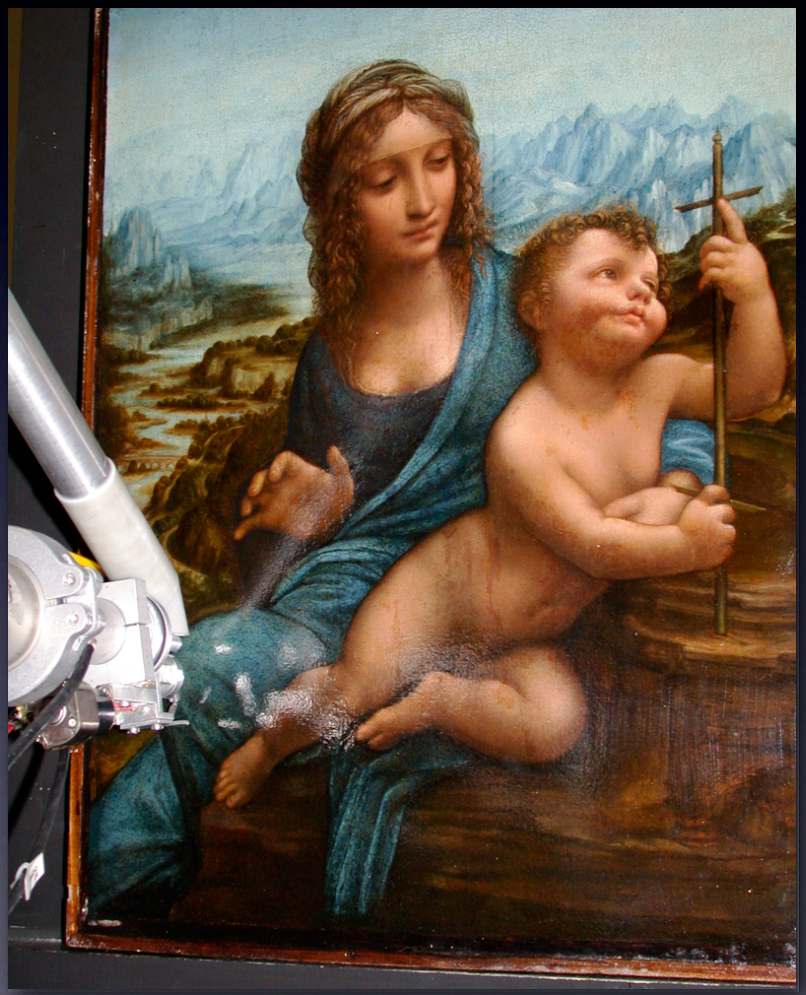

"Maddonna dei fusi", Leonardo da Vinci (1501)

Lapis-lazuli is a blue pigment, mainly composed of lazurite ($3Na_2O \cdot 3Al_2O_3 \cdot 6SiO_2 \cdot 2Na_2S$)

Limited possibility of identifying lapis-lazuli by PIXE in canvas and wood paintings:

- *low-energy X-rays absorption in the varnish and in the paint layer itself*
- *signal interference from other pigments*

Lapis-lazuli pigment in paint layers

PIXE spectra

PIGE spectra

Original

Blue pigment mixed with Lead white (Ca and Fe from the varnish)

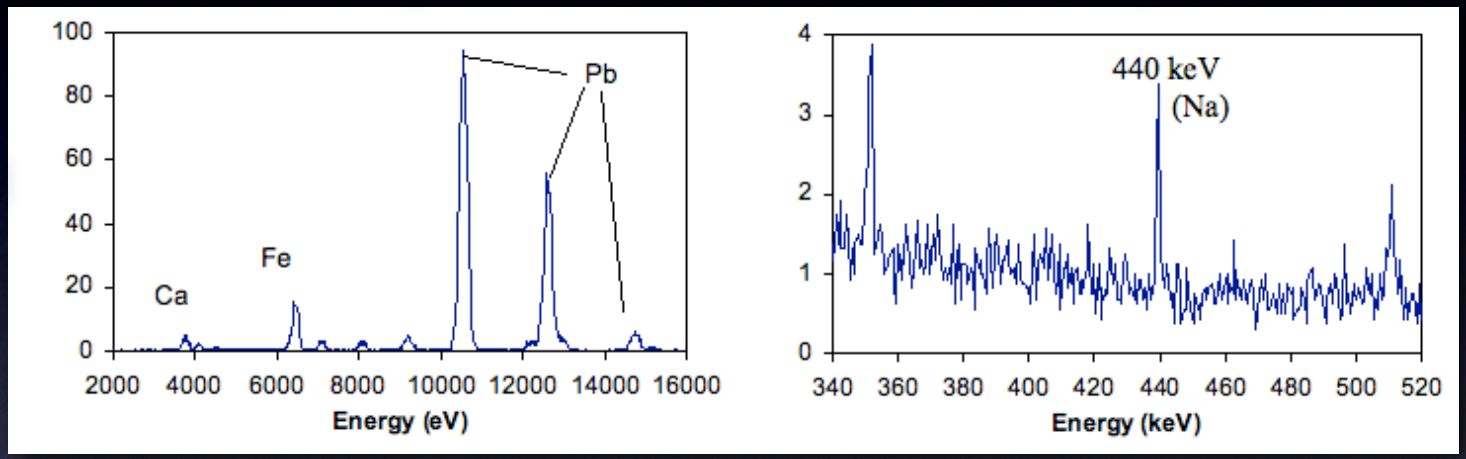

Restored

Cobalt blue and Zinc white (used only from XIX century!)

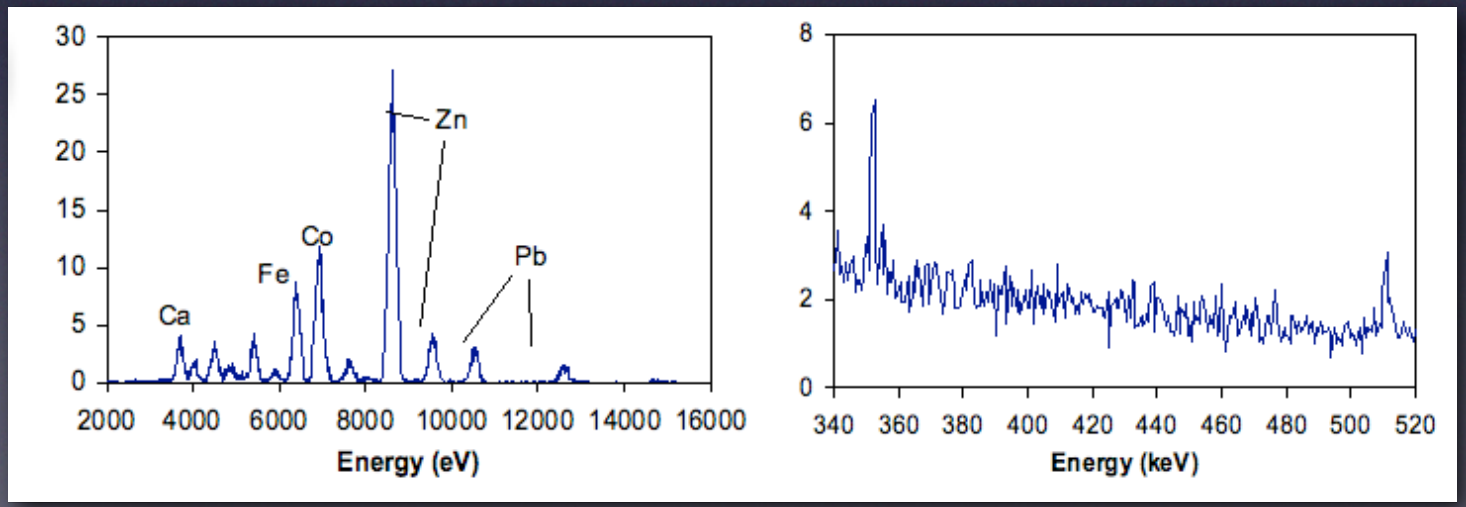

Analysis of ancient Roman glasses

Roman glass mosaic *tesserae* from Villa Adriana, Tivoli (Italy)

Quantification of Na is of great importance for the characterizaztion of ancient glasses

Two basic typologies of Western glass:

- **natron** (high Na_2O, low K_2O and MgO)
  Roman and High Middle Ages
- **plant ash** (low Na_2O, high K_2O)
  since Middle Ages

Sodium in Roman glasses

X-rays fom the lightest elements strongly absorbed by crusts and *patinae*

Roman glass mosaic *tesserae*

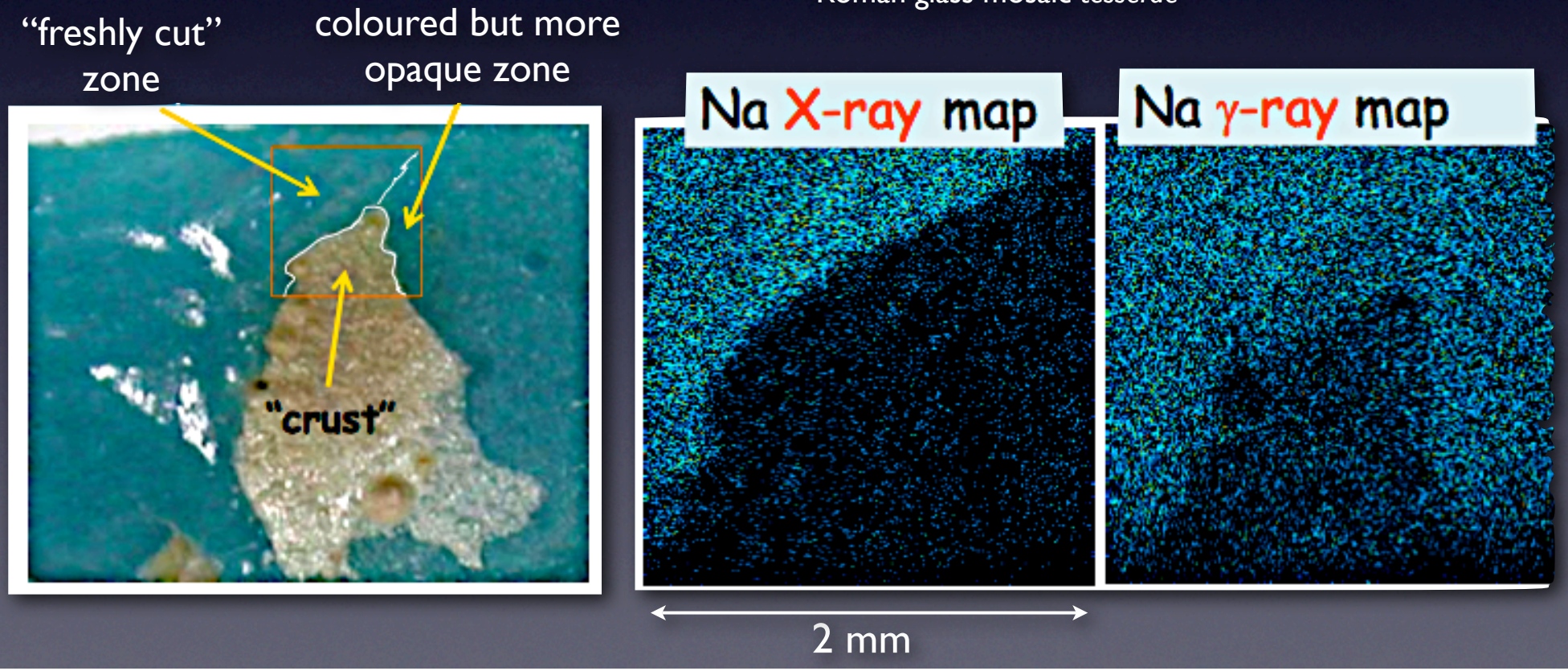

Sodium in Roman glasses

PIXE spectra PIGE spectra

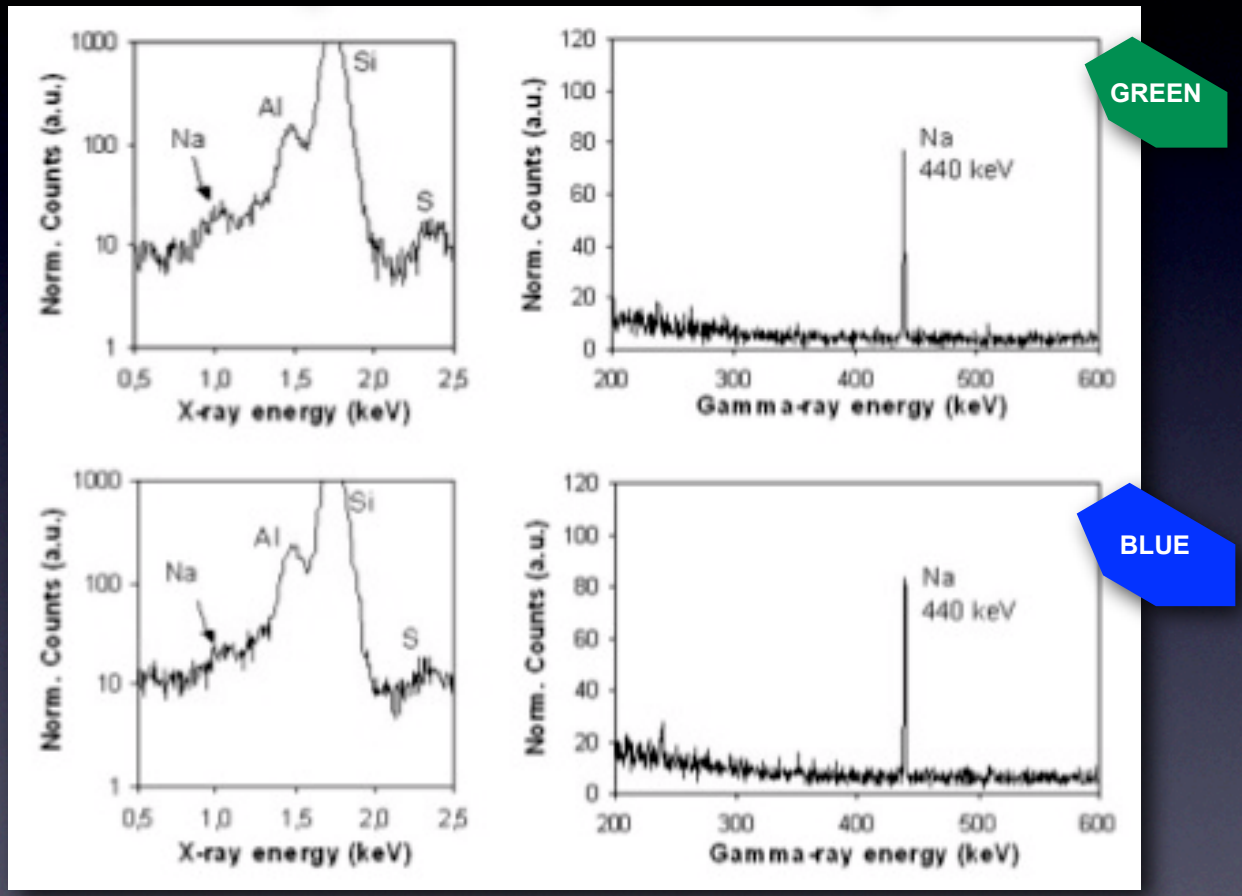

X-rays from the lightest elements strongly absorbed by crusts and *patinae*

Sodium in Roman glasses

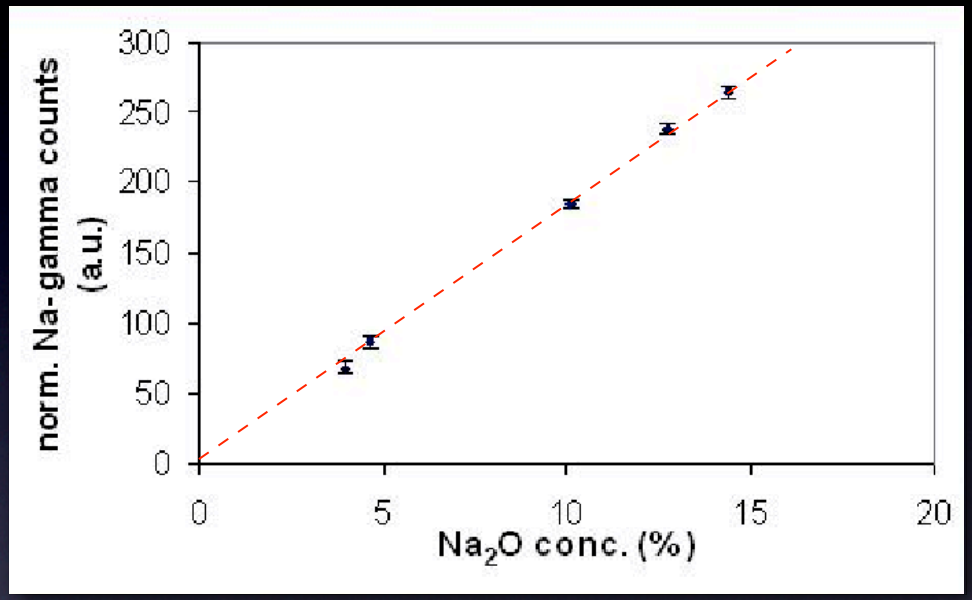

Estimate of Na content by comparing gamma-ray yields to those of thick glass standards (NIST SRM) with certified Na_2O concentration

Concentration ranges perfectly compatible with the typical Roman soda-lime-silica glass

glass colour	main oxides (%)			
	Na_2O	SiO_2	CaO	PbO
green	~20	55-60	5-9	1-3
blue	~20	60-65	5-9	<0.1
turquoise	~20	55-60	5-9	<0.3
yellow	~15	55-60	5-9	5-8
red	~10	35-40	5-9	30-35

RBS: External vs Vacuum

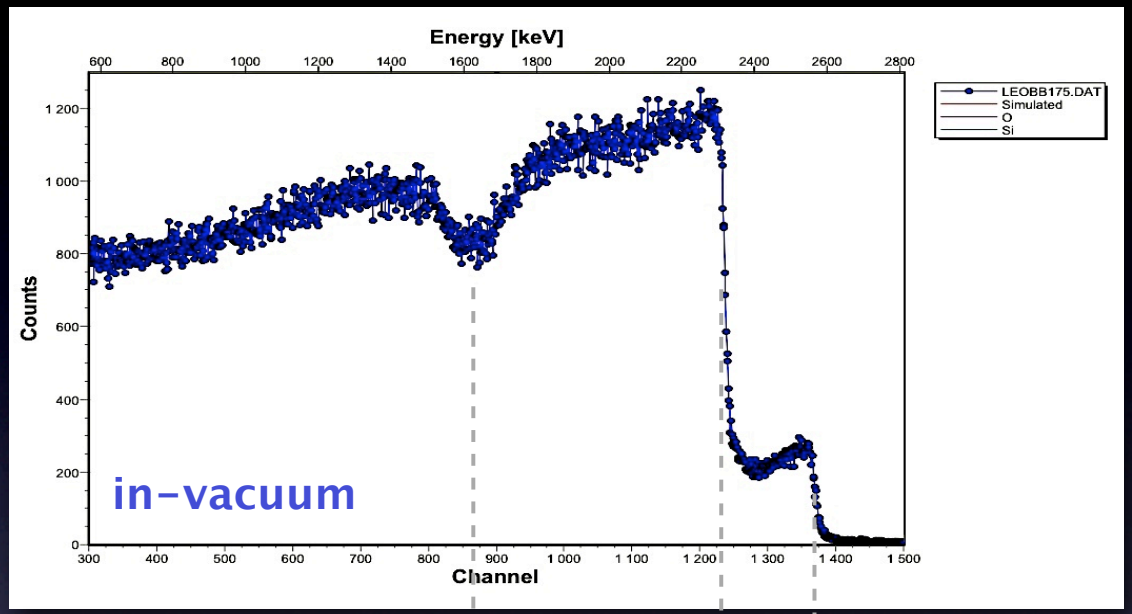

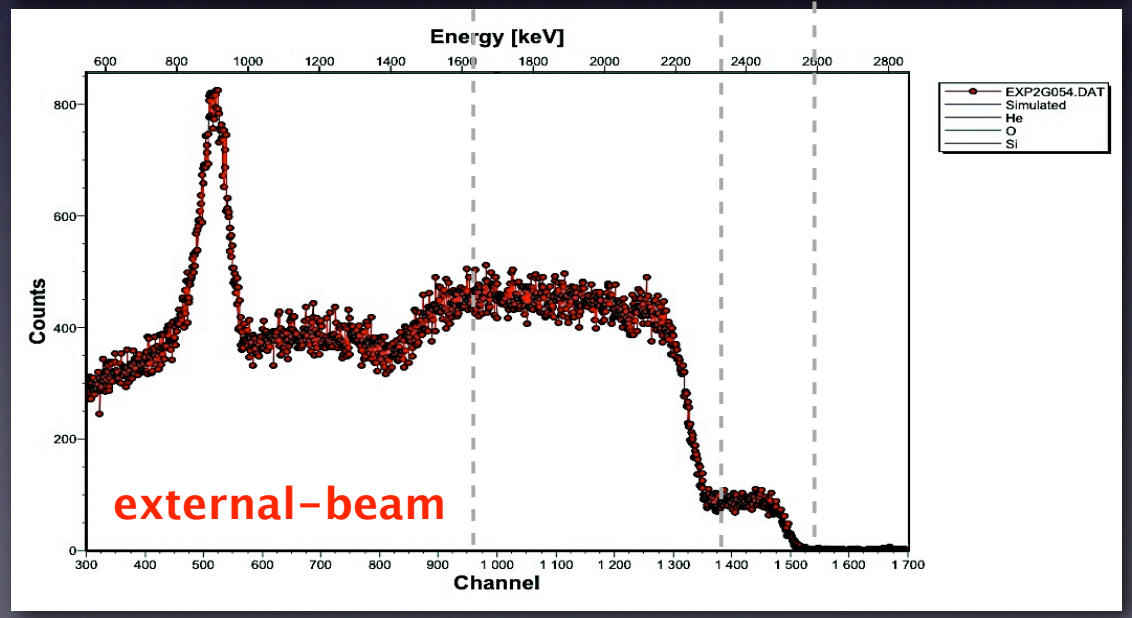

- *3 MeV protons on target*
- *θ = 150°*
- *SiO_2 target*

- Energy loss and energy straggling * in exit window and external path in atmosphere

* 15 keV FWHM for 500 nm Si_3N_4 + 10 mm He

Gold alloy or gilding

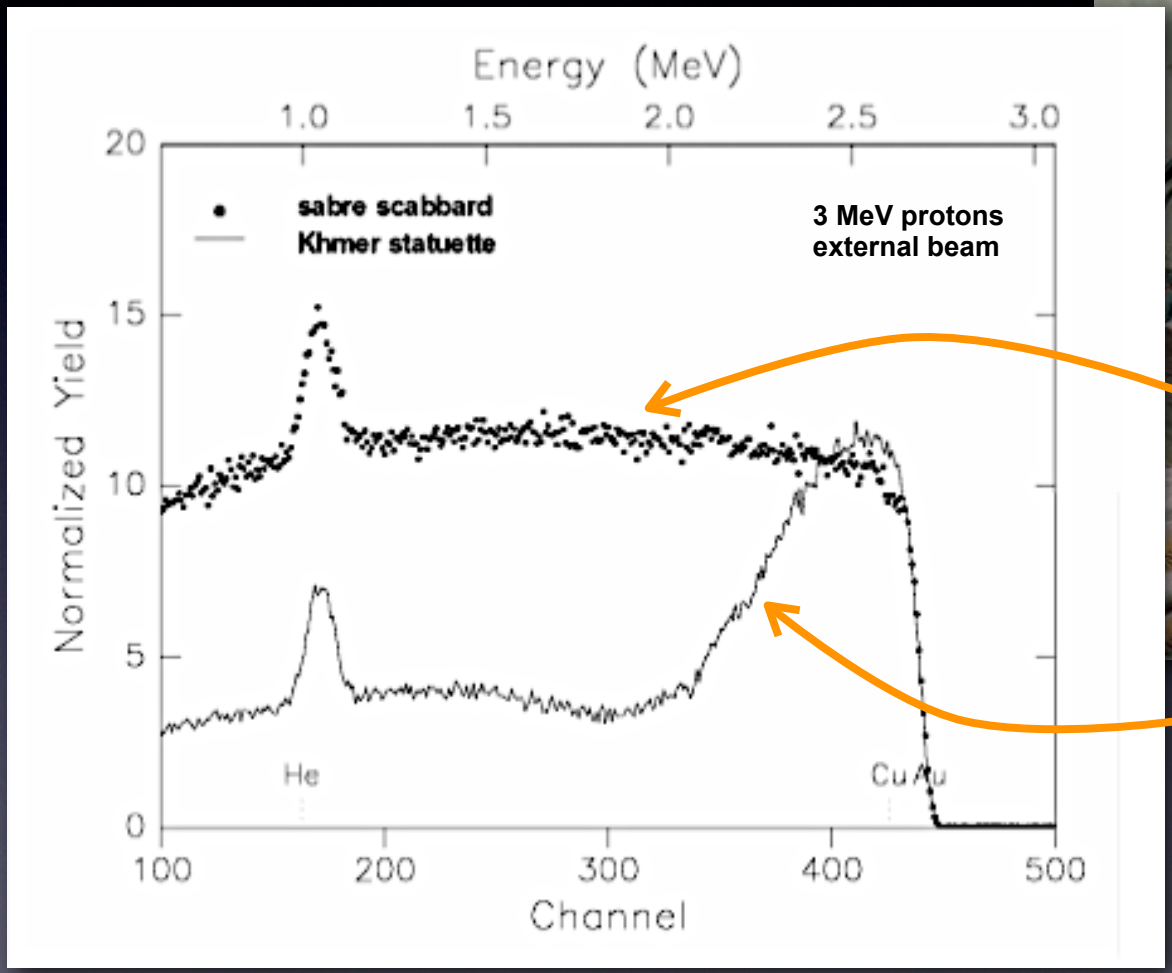

The scabbard is made of a thick Au-Cu alloy (thickness > 10 μm).

For comparison, the gilding of the statuette is about 2 μm thick.

From the width of the Au signal it is possible to obtain the thickness of the gilding (*dE/dx* is known).

RBS analysis of a gilded bronze chandelier (XI century) from the Cathedral of Hildesheim, Germany

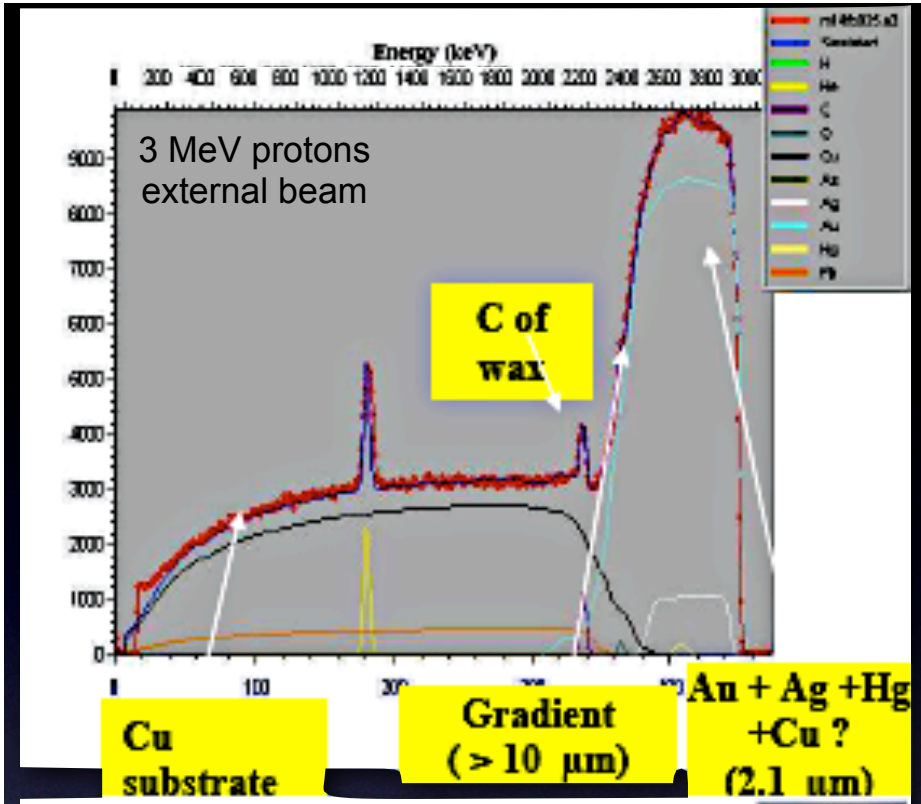

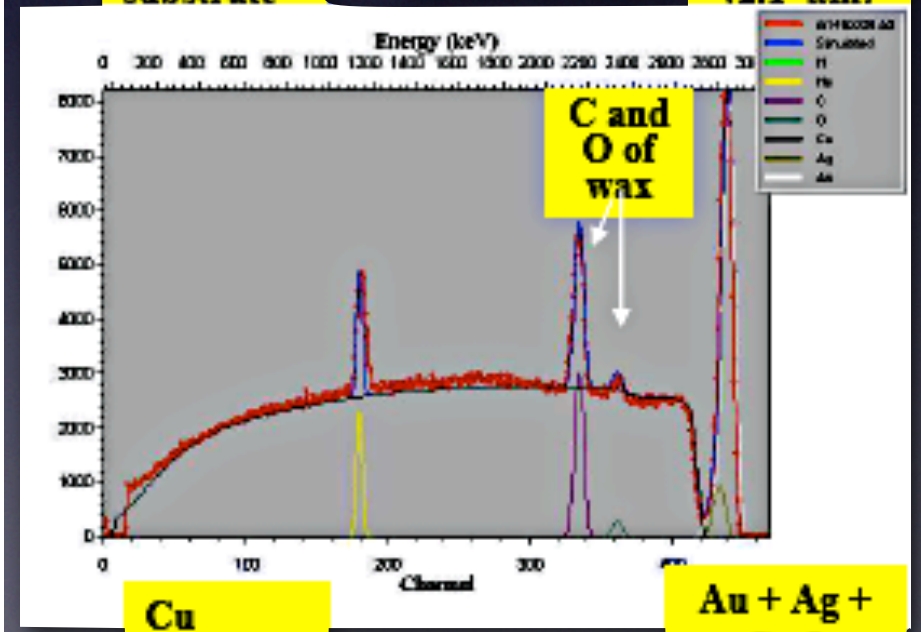

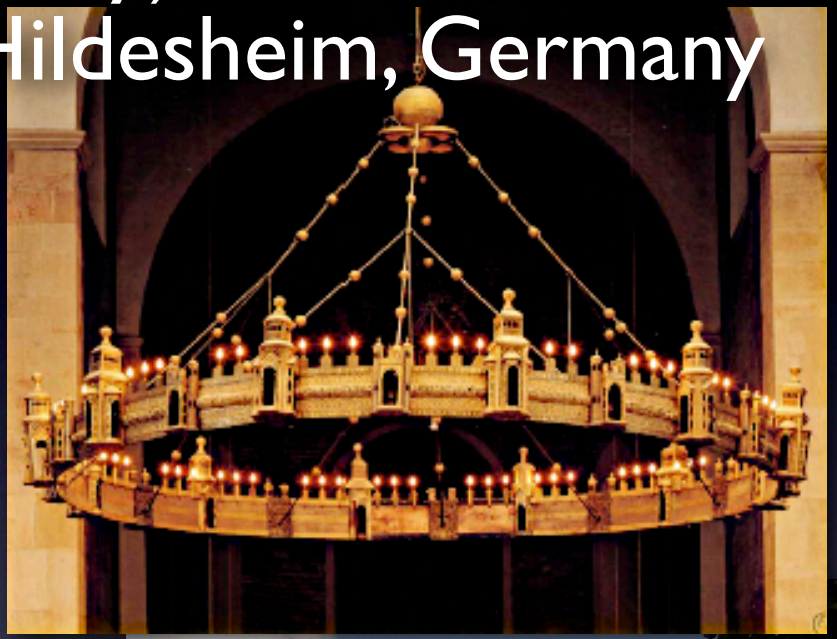

RBS study of glass corrosion

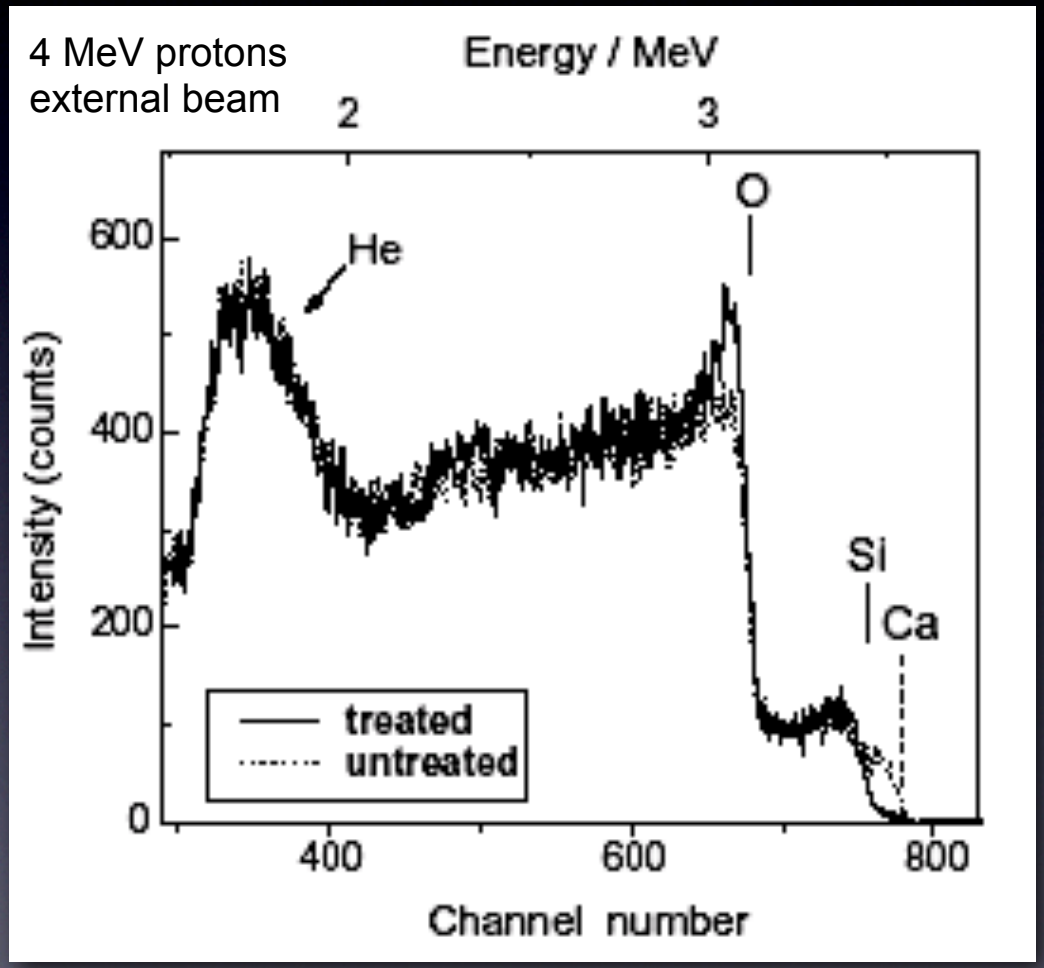

Leaching of Ca, K, Na from the interaction with moisture or water and formation of surface hydrate silicates
(cfr. PIGE analysis)

Complementary PIXE/RBS

In samples with a layered structure the elemental depth profile is needed to correctly calculate absorption effects in PIXE

PIXE strenghts

- High sensitivity
- Excellent specificity

RBS weaknesses

- Low sensitivity
- Poor mass resolution

RBS strenghts

- Traceable accuracy
- Excellent depth resolution

PIXE weaknesses

- Poor traceability
- Poor depth resolution

Characterization of paint layers by simultaneous PIXE/RBS analysis

"La Bohémienne", Frans Hals (1630)

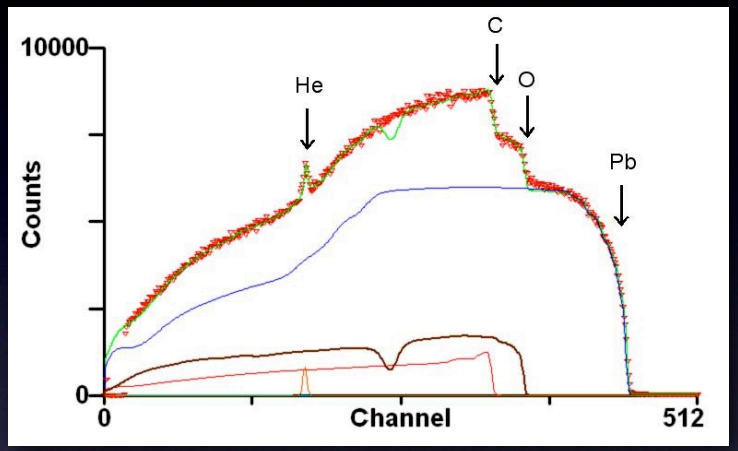

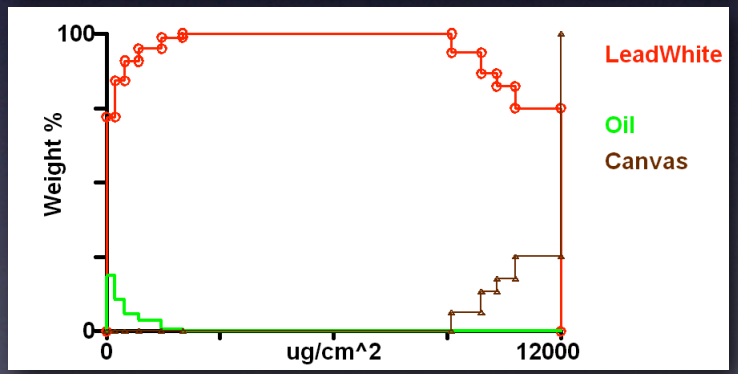

The canvas is schematized as carbon plus chalk ($CaCO_3$)

Ochre pigment (ematite) detected and quantified thanks to simultaneous PIXE/RBS measurements: $440 \cdot 10^{15}$ atoms/cm^2 Fe_2O_3 in $7000 \cdot 10^{15}$ atoms/cm^2 of oil ($C_{13}O_5$)

Thanks for
your attention!

Bibliography

- R. Tesmer, M. Nastasi ed.s *"Handbook of Modern Ion Beam Materials Analysis"* MRS
- S. A.E. Johansson, J.L. Campbell, K.G. Malmqvist ed.s *"Particle-induced X-ray emission spectrometry (PIXE)"* John Wiley & sons
- W.-K. Chu, J.W. Mayer, M.-A. Nicolet *"Backscattering Spectrometry"* Academic Press
- G. Deconninck et al. *"Prompt gamma-ray spectroscopy and its use in elemental analysis"* At. Energy Rev. suppl. no. 2 (1981) 151